(2)

US Army Corps of Engineers

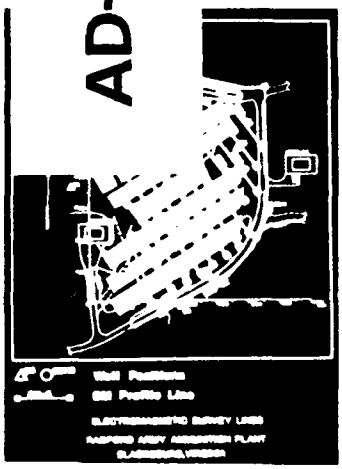

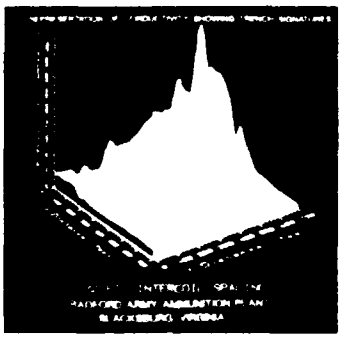

GEOTECHNICAL LABORATORY

MISCELLANEOUS PAPER GL-89-18

GEOPHYSICAL INVESTIGATION AT HAZARDOUS WASTE MANAGEMENT SITE 16 RADFORD ARMY AMMUNITION PLANT RADFORD, VIRGINIA

by

José L. Llopis, Keith J. Sjostrom

Geotechnical Laboratory

DEPARTMENT OF THE ARMY
Waterways Experiment Station, Corps of Engineers
3909 Halls Ferry Road
Vicksburg, Mississippi 39180-6199

September 1989
Final Report

Prepared for US Army Engineer District, Fort Worth
Fort Worth, Texas 76102-0300

Destroy this report when no longer needed. Do not return it to the originator.

The findings in this report are not to be construed as an official Department of the Army position unless so designated by other authorized documents.

The contents of this report are not to be used for advertising, publication, or promotional purposes. Citation of trade names does not constitute an official endorsement or approval of the use of such commercial products.

Unclassified

SECURITY CLASSIFICATION OF THIS PAGE

REPORT DOCUMENTATION PAGE

Form Approved OMB No. 0704-0188

1a REPORT SECURITY CLASSIFICATION: Unclassified	1b RESTRICTIVE MARKINGS
2a SECURITY CLASSIFICATION AUTHORITY	3 DISTRIBUTION/AVAILABILITY OF REPORT: Approved for public release; distribution unlimited.
2b DECLASSIFICATION/DOWNGRADING SCHEDULE	
4 PERFORMING ORGANIZATION REPORT NUMBER(S): Miscellaneous Paper GL-89-18	5 MONITORING ORGANIZATION REPORT NUMBER(S)
6a NAME OF PERFORMING ORGANIZATION: USAEWES Geotechnical Laboratory; 6b OFFICE SYMBOL (If applicable): CEWES-GG-F	7a NAME OF MONITORING ORGANIZATION
6c ADDRESS (City, State, and ZIP Code): 3909 Halls Ferry Road, Vicksburg, MS 39180-6199	7b ADDRESS (City, State, and ZIP Code)
8a NAME OF FUNDING/SPONSORING ORGANIZATION: US Army Engineer District, Fort Worth; 8b OFFICE SYMBOL (If applicable): CESWF	9 PROCUREMENT INSTRUMENT IDENTIFICATION NUMBER: IAO No. E87870129
8c ADDRESS (City, State, and ZIP Code): 819 Taylor Street, Fort Worth, TX 76102-0300	10 SOURCE OF FUNDING NUMBERS: PROGRAM ELEMENT NO; PROJECT NO; TASK NO; WORK UNIT ACCESSION NO

11 TITLE (Include Security Classification): Geophysical Investigation at Hazardous Waste Management Site 16, Radford Army Ammunition Plant, Radford, Virginia

12 PERSONAL AUTHOR(S): Llopis, Jose L., Siostrom, Keith J.

13a TYPE OF REPORT	13b TIME COVERED	14 DATE OF REPORT (Year, Month, Day)	15 PAGE COUNT
Final report	FROM Feb 87 TO Mar 87	September 1989	56

16 SUPPLEMENTARY NOTATION: Available from National Technical Information Service 5285 Port Royal Road, Springfield, VA 22161.

17 COSATI CODES			18 SUBJECT TERMS (Continue on reverse if necessary and identify by block number)
FIELD	GROUP	SUB-GROUP	Electromagnetic induction; Seismic refraction; Geophysical investigation; Hazardous waste

19 ABSTRACT (Continue on reverse if necessary and identify by block number)

This report describes procedural details and test results of a geophysical investigation conducted at Hazardous Waste Management Site-16 (HWMS-16), Radford Army Ammunition Plant, VA. The geophysical investigation, part of a comprehensive ground-water assessment program, was conducted to obtain subsurface information regarding HWMS-16, thus aiding in determining the most optimal locations for future monitoring wells. The two geophysical methods used in this investigation were electromagnetic (EM) induction and seismic refraction. A number of anomalous areas including a suspected sinkhole were discerned at HWMS-16. Also, the EM method proved to be effective in delineating the boundries of covered and leveled-off landfill cells and distinguishing landfill cells used for the disposal of household waste from those used for the disposal of hazardous waste.

20 DISTRIBUTION/AVAILABILITY OF ABSTRACT	21 ABSTRACT SECURITY CLASSIFICATION	
☒ UNCLASSIFIED/UNLIMITED ☐ SAME AS RPT ☐ DTIC USERS	Unclassified	
22a NAME OF RESPONSIBLE INDIVIDUAL	22b TELEPHONE (Include Area Code)	22c OFFICE SYMBOL

DD Form 1473, JUN 86 Previous editions are obsolete

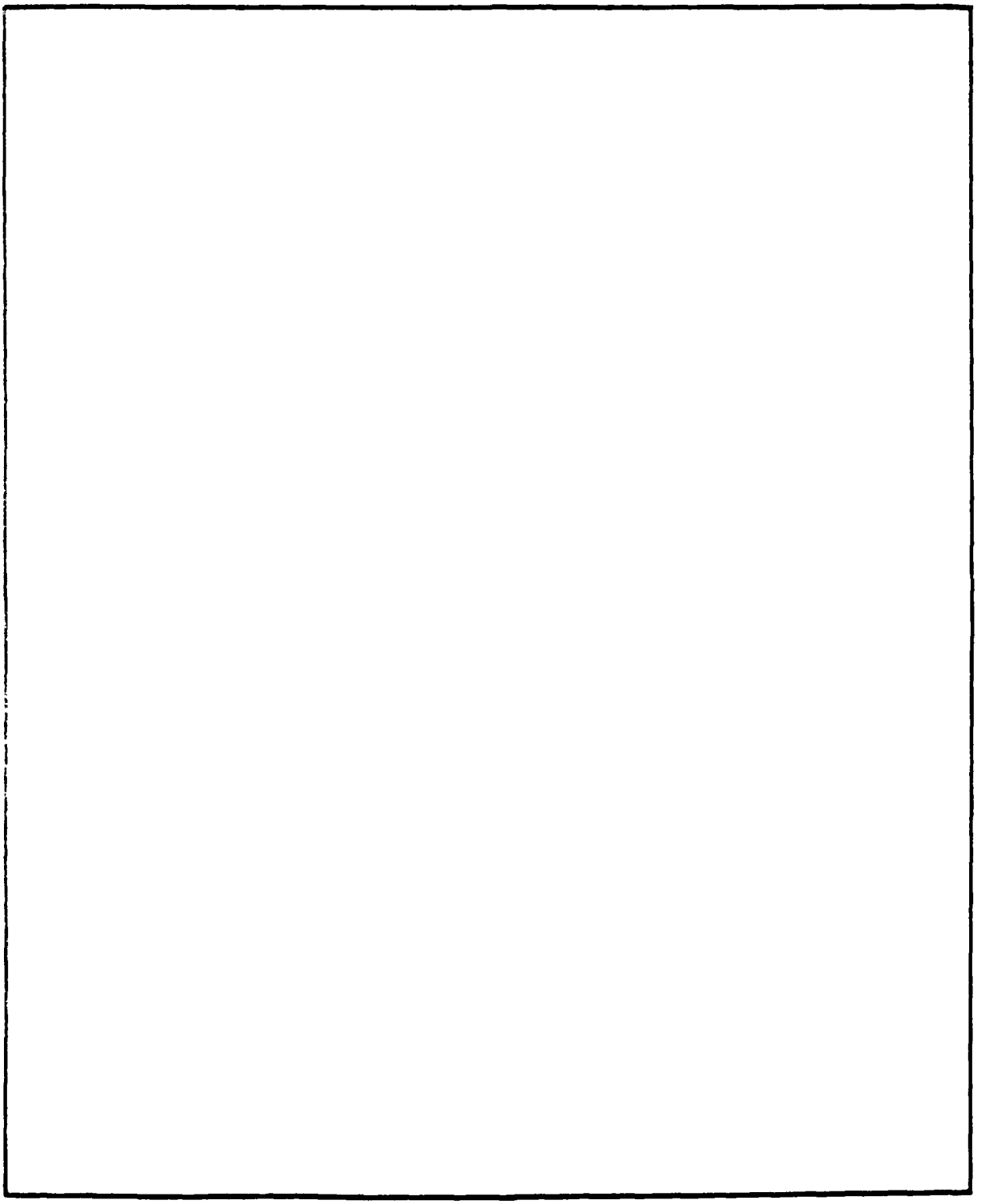

PREFACE

A geophysical investigation at Radford Army Ammunition Plant was authorized by the US Army Engineer District, Fort Worth, under IAO No. E87870129 dated 23 January 1987.

This report was prepared by Messrs. José L. Llopis and Keith J. Sjostrom, Earthquake Engineering and Geosciences Division (EEGD), Geotechnical Laboratory (GL), US Army Engineer Waterways Experiment Station (WES), under the direct supervision of Mr. Joseph R. Curro, Jr., EEGD. The work was done under the general supervision of Drs. A. G. Franklin, Chief, EEGD, and William F. Marcuson III, Chief, GL.

The field work was performed during the period 26 February through 6 March 1987 by Messrs. José L. Llopis, Keith J. Sjostrom, and Donald H. Douglas, EEGD. Mr. Charlie H. Whitten, EEGD, provided invaluable technical support for this investigation.

Commander and Director of WES during the preparation of this report was COL Larry B. Fulton, EN. Dr. Robert W. Whalin was the Technical Director.

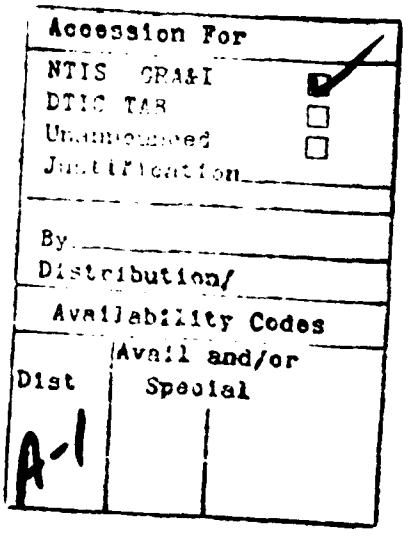

CONTENTS

CONVERSION FACTOR, NON-SI TO SI (Metric) UNITS OF MEASUREMENT

Non-SI units of measurement used in this report can be converted to SI (Metric) units as follows:

Multiply	By	To Obtain
feet	0.3048	metres
miles (US statute)	1.609347	kilometres
millimhos per foot	3.28	millimhos per metre
ohm-ft	0.3048	ohm-metres

GEOPHYSICAL INVESTIGATION AT HAZARDOUS WASTE MANAGEMENT SITE 16, RADFORD ARMY AMMUNITION PLANT, RADFORD, VIRGINIA

PART I: INTRODUCTION

Background

1. Radford Army Ammunition Plant (RAAP) is located in southwestern Virginia approximately 47 miles southwest of Roanoke and approximately 7 miles* southwest of Blacksburg, Virginia (Figure 1). The primary mission of the contractor operated RAAP is to manufacture a variety of propellants and explosives as directed by the US Army. As a result of these manufacturing processes, some waste materials are stored in man-made lagoons and other wastes in landfills (hazardous waste management sites). In compliance with the Resource Conservation and Recovery Act (RCRA) of May 1980, a drilling program was initiated in April 1981 by the US Army Environmental Hygiene Agency (USAEHA) to establish ground water monitoring wells in the vicinity of hazardous waste management sites at RAAP.

Objectives

2. The U.S. Army Engineer Waterways Experiment Station (WES) conducted a geophysical survey at Hazardous Waste Management Site-16 (HWMS-16) to aid in determining the optimal locations for future monitoring wells (Figure 2). The objectives of the geophysical field program were to map any anomalous subsurface conditions existing at the site and to determine the existence of a suspected sink hole. Electromagnetic (EM) and seismic refraction methods were the two geophysical techniques used to meet the above objectives. Another objective of this investigation was to determine the effectiveness of the EM technique as a "tool" in delineating individual landfill cells known to exist at HWMS-16.

---

* A table of factors for converting non-SI to SI (metric) units of measurement is presented on page 3.

PART II: GEOLOGY

Physiography and Regional Geology

3. The RAAP lies within the Valley and Ridge physiographic province of the Appalachian Highland region of North America. The topography of the area is characterized by elongate northeast-southwest trending ridges and valleys. The Valley and Ridge province is comprised of complexly folded and thrust faulted sedimentary rocks ranging in age from Cambrian through Pennsylvanian. Because of differential weathering, the relatively more resistant sandstone and dolomites have yielded ridges while the less resistant shales and limestones have weathered into valleys and sinkholes (Aycock 1987).

Site Geology

4. The area comprising HWMS-16 is covered by alluvium consisting of sand, silt, and gravel and ranging in thickness between approximately 30 and 80 ft. Underlying the alluvium is a layer of residuum, the in-situ product of bedrock weathering. The residuum consists generally of yellow-tan, silty-clay to clayey-silt material, with traces of sand. The thickness of the residuum varies between approximately 1 and 35 ft. Underlying the residuum at HWMS-16 is the Rome Formation, "bedrock", consisting chiefly of interbedded limestone and shale. Borings placed in the vicinity of HWMS-16 show the presence of brecciated rock with angular fragments of limestone, dolomite, and shale in a matrix of greenish siltstone and claystone indicating a possible fault in the area (Porter and Sipher 1984). The brecciated material may act as a conduit for contaminant transport.

PART III: GEOPHYSICAL METHODS

Electromagnetic Surveys

5. The EM technique is used to measure differences in terrain conductivity. Like electrical resistivity, conductivity is affected by differences in soil porosity, water content, chemical nature of the ground water and soil, physical nature of the soil, etc. In fact, for a homogeneous earth the true conductivity is the reciprocal of the true resistivity. Some advantages of using the EM over the resistivity technique are (a) less sensitivity to localized resistivity inhomogeneities, (b) no direct contact with the ground required, thus no current injection problems, (c) smaller crew size required, and (d) rapid measurements (McNeil 1980).

6. The EM equipment used at HWMS-16 consists of two coils connected by a cable. One coil is a transmitter and the other coil is a receiver. The transmitter coil (energized with an alternating current (AC) at an audio frequency) is placed on the ground surface and the receiver coil placed a small distance away (33, 66, or 132 ft). The transmitter coil creates a time-varying magnetic field which induces small eddy currents in the ground. These currents then generate a secondary magnetic field which is sensed together with the primary field by the receiver coil. The measurements, in millimhos per foot (mmhos/ft), are then presented in profile plots or as isoconductivity contours if data are obtained in a grid form. A more thorough discussion on EM theory and field procedures is given by Butler (1986) and Telford et al. (1973).

7. Figure 3 shows the location of the twelve EM survey lines conducted at HWMS-16. All the EM lines were run using intercoil separations of 33, 66, and 132 ft. Analogous to resistivity profiling, the greater the coil separation, the greater the depth of investigation. All measurements were taken in the horizontal dipole mode (coils oriented vertically and coplanar). Readings for each survey line, with the exception of survey line EM-12, were obtained with the coil orientation perpendicular to the strike of the survey lines i.e, a coil on either side of the survey line axis. In addition, lines EM-1 through EM-6 were run with the coils oriented parallel to the survey lines (coils parallel to the strike of the survey line). The two different coil

orientations (perpendicular and parallel to the strike of the survey line) were conducted to assess which orientation would better resolve the individual landfill cell boundaries. Survey lines EM-1 through -11 were spaced 50 ft apart. Readings were taken at 20 ft intervals along each survey line except for line EM-12 in which readings were taken every 25 ft.

Seismic Refraction Surveys

8. The seismic refraction method utilizes the fact that the compression-wave (P-wave) velocity of a material is dependent on its elastic properties. It is based on the assumption that materials are locally homogeneous and isotropic. In the seismic refraction method, energy is imparted into the ground usually by means of explosives or by striking a metal plate on the ground with a sledgehammer to produce a seismic disturbance. The location of the seismic disturbance is considered to be a point source and the disturbance is transmitted through the ground as a series of waves. In this investigation the P-wave will be the elastic wave studied. Geophones are implanted in the ground surface along a straight line spaced at regular intervals. The length of the survey line depends on the depth of the investigation. A common rule of thumb is that the length of the line should be three to four times the depth of interest. Interpretation of seismic refraction data consists of plotting the P-wave arrival time to each geophone versus the respective geophone distance from the seismic source. The slope of the straight line segments drawn through the points correspond to the P-wave velocities of the materials. With further analysis, the depths to the interfaces with contrasting velocities can be determined.

9. Figure 4 shows the location of refraction lines R-1 through R-7 which were run at HWMS-16. Refraction lines R-2 through R-6 consisted of 24 geophones spaced 15 ft apart with shot points offset 15 ft from the end of each line thus, giving a total line length of 375 ft. This length provides a maximum depth of investigation of approximately 90 to 120 ft. Refraction lines R- 1 and R-7 consisted of 24 geophones spaced 10 ft apart with shot points offset 10 ft from the end of the lines thus, giving an end-to-end survey line length of 250 ft. Hence, the 250-ft refraction lines are useful in determining the velocities to a maximum depth of approximately 60 to 80 ft.

The surveys were conducted using a portable 24-channel seismograph and stored on magnetic tape for subsequent processing and interpretation. Energy was imparted into the ground by the use of two-component explosives. A more thorough discussion of seismic refraction field procedures are given in Department of the Army (1979).

PART IV: RESULTS

Electromagnetic Surveys.

10. Results of EM surveys EM-1 through -11 are presented in two fashions, two dimensional (2-D) and three dimensional (3-D) views. Figures 5 through 7 present a 2-D view of the data obtained from EM survey lines EM-1 through -11 for intercoil spacings of 33, 66, and 132 ft, respectively. Figures 8 through 10 present a 3-D view of the EM data for lines EM-1 through -11 with intercoil spacings of 33, 66, and 132 ft, respectively. Figures 5 through 10 correspond to the case where the coil orientation is perpendicular to the strike of the EM survey line. Referring to Figure 5, 33 ft intercoil surveys, three prominent conductivity highs can be seen occurring at the approximate x-y coordinates (450,625), (325,375), and (200,175). Referring to Figures 6 and 7, 66 and 132 ft intercoil surveys, respectively, it can be seen that the anomalously high conductivity reading at (450,625) becomes less prominent. The area with the anomalously high conductivity values located at (450,625) occurs on the landfill boundary and may be due in part to buried man-placed material and in part to natural conditions, such as higher water content or more clayey material. It is also possible that the conductivity high at (450,625) may be caused by a septic tank which, according to reference drawings, is buried in the vicinity. It is not known whether the septic tank is made of concrete or steel therefore, it is difficult to assess its influence on the conductivity readings. The other two conductivity highs which occur in the landfill are believed to be caused by (1) electrically conductive slag-type material used as cover material at the site and/or (2) the waste. Referring to Figures 8 through 10, 3-D perspectives for EM surveys with intercoil spacings of 33, 66, and 132 ft, respectively, a series of linear northeast-southwest trending features can be discerned. These more conductive linear features apparently correspond with waste trenches known to exist in the area. It is noted that the linear feature with the highest conductivity values corresponds to a landfill trench (cell #4) which was used for the burial of hazardous waste. The remaining trenches reportedly contain sanitary waste and have relatively lower conductivity readings.

11. Figures 11 through 13 show the interpreted locations of the landfill cells based on the 33, 66, and 132 ft perpendicularly oriented EM survey data, respectively. The "actual" cell locations referred to in Figures 11 through 13 are close approximations of the landfill locations. The precise locations of the landfill cells are not known because they were filled and leveled off prior to the time they were surveyed in 1983. The locations of the actual landfill cells as shown in Figures 11 through 13 are based on reference drawings dated 7 February 1983 provided by RAAP personnel. The locations of the landfills were interpreted from the EM data as areas having a relative high conductivity. Referring to Figures 11 through 13 it can be seen that the interpreted locations of the landfill cells correspond well in terms of width, length, and orientation with the actual locations. Also it will be noted that there is not much difference in the interpretations between the 33, 66, and 132 ft intercoil spacing EM surveys.

12. Figures 14 through 16 show a 2-D view of the EM data obtained with coils oriented parallel to the EM survey lines for intercoil spacings of 33, 66, and 132 ft, respectively. Referring to Figure 14, two conductivity highs are apparent; one is centered at approximate coordinate (290,350) and the other at (150,150). Referring to Figure 15 (66 ft intercoil spacing) conductivity anomalies can also be discerned in the same general locations as for the 33 ft case, Figure 14. However, the anomalies are broader and less distinct. Referring to Figure 16 (132 ft intercoil spacing) it can be seen that there is little variation in conductivity across the site, when compared to the data in Figures 14 and 15, intercoil spacings of 33 and 66 ft, respectively. Referring to Figures 17 through 19, 3-D perspectives for EM surveys with intercoil spacings of 33, 66, and 132 ft, respectively, it can be seen that the 66 ft intercoil spacing survey best defines the landfill cells.

13. Interpreted locations of the landfill cells, based on the results of the EM survey conducted parallel to the strike of the EM lines for the 33, 66 and 132 ft intercoil spacings, are presented in Figures 20 through 22, respectively. The locations of the landfills were interpreted as being areas having a relatively high conductivity. It can be seen in Figures 20 through 22 that these surveys have less resolving power for delineating the cells than when the survey is conducted perpendicular to the EM lines (parallel to the

strike of the cells). The 66 ft intercoil spacing survey (Figure 21) defined the location of the cells better than the did the 33 or 132 ft surveys (Figures 20 and 22, respectively).

14. The advantage of conducting the EM surveys with the coils oriented vertically and coplanar are that the coils are not as sensitive to misalignment and therefore the survey proceeds more rapidly. However, when the survey is conducted in this manner, readings taken are affected greatly by near-surface materials thus masking changes in conductivity at greater depths. The "two-spacing" technique described by McNeil (1985) was used to determine whether soil conductivity was increasing or decreasing with depth. For this technique intercoil spacings of 33 and 66 ft and/or 66 and 132 ft were used to conduct the survey. For the case where 33 and 66 ft intercoil spacings are used, apparent conductivity readings for 33 ft and 66 ft spacings, designated C33 and C66, are taken at each measurement station. Also, at each measurement station a new apparent conductivity, designated Cn, is computed as follows:

$$Cn = 2*C66 - C33$$

The apparent conductivities (Cn) obtained from performing the above computation are plotted in 2-D. The plot for the 33 ft intercoil spacing (C33) gives the conductivity response of materials for depths of less than approximately 13 ft while the data of Cn gives the conductivity response at depths greater than 13 ft. When the survey is conducted with intercoil spacings of 66 and 132 ft then the plot for C66 gives the conductivity response of materials at depths less than 26 ft while the plot of 2*C132 - C66 gives the conductivity response at depths greater than 26 ft. For example, if Cn is equal or less than 0 then the conductive material is very close to the surface. If Cn is equal to C33 then the conductivity is constant with depth, and if Cn is greater than C33 then the conductivity increases with depth. Similarly, the same holds true for the case where the 132- and 66-ft intercoil spacings are used. When 2*C132 - C66 is less than zero then the conductive material is very close to the surface, if 2*C132 - C66 is equal to C66 then the conductivity is constant with depth, and if 2*C132 - C66 is greater than C66 then the conductivity increases with depth.

15. Figures 23 and 24 are plots of the EM "two-spacing" technique, Cn and 2*C132 - C66, respectively, run with the coils oriented perpendicular to the axis of the EM survey lines. A comparison of Figure 23 with Figure 5 (respective 2-D plot of C33) suggests that the conductive material is near the surface since values in Figure 23 are consistently lower than those in Figure 5. Comparison of Figure 24 with Figure 6 (respective 2-D plot of C66) also shows that conductivity is decreasing with depth.

16. Figures 25 and 26 are plots of the EM two spacing technique, Cn and 2*C132-C66, respectively, run with the coils oriented parallel to the axis of the EM survey lines. Figure 25 indicates negative zones centered on approximately (175,175) and (275,350). When Figure 25 is compared with Figure 14 (respective 2-D plot of C33) these two zones can be interpreted as areas with very conductive material near the ground surface since the values of Cn (Figure 25) in these areas are less than the values for C33 (Figure 14). Referring to Figure 26 a negative zone is noted occurring around approximate coordinate (300,350) while Figure 15, which is the corresponding 2-D plot of C66, indicates a conductivity high in the same area. This again indicates that the more conductive material is near the surface.

17. Figure 27 presents the results of the EM profile line conducted around the perimeter of HWMS-16, along the road as shown in Figure 3. Referring to Figure 27, anomalous areas are noted centered at approximately 50 ft and 650 ft. The anomalies are characterized by a peak bounded by a trough on either side. These anomalies may be indicative of a subsurface, conductive, contaminant plume.

Seismic Refraction Surveys

18. Figures 28 through 34 present the time versus distance (TD) information obtained from running seismic refraction surveys R-1 through -7, respectively. It will be noted that due to the disturbed nature of the site caused by trenching and backfilling, the site is quite inhomogeneous thus, making depth and velocity determinations difficult. Presented below are interpretations based on the seismic refraction technique using geophysical and geological judgment. Referring to Figure 28, line R-1, two velocity layers are represented. The uppermost layer has a velocity of 2050 fps while

the lower velocity layer, occurring at depths ranging between 34 and 54 ft has a velocity of 6910 fps. Referring to Figure 29, line R-2, two layers with velocities of 1550 and 11,190 fps are detected below the southwestern portion of the line while three layers having velocities of 1520, 2510, and 8620 fps are interpreted at the northeastern end of the line. The depth to the 11,190 fps layer beneath the southwestern shotpoint is 48 ft while the depths to the 2510 and 8620 fps layers are 16 and 55 ft, respectively. It appears that the 8620 and 11,190 fps layer correspond to the same material (bedrock). It also appears that the 2510 fps layer "pinches out" to the southwest. Referring to Figure 30, line R-3, two layers with velocities of 1970 and 8930 fps are discerned at the southwestern end of the line while three layers with velocities of 1650, 4520, and 10,710 fps are detected at the northeastern part of the line. The average velocity of the uppermost layer is 1810 fps while the true velocity of the bedrock is 9740 fps and is detected at depths ranging between 54 and 87 ft. The 4520 fps layer which is detected at a depth of 33 ft, beneath the northeastern shot point, is believed to thin out towards the southwest. Figure 31 presents the TD information obtained from running survey line R-4. Three velocity layers were interpreted from this survey line. The first layer has a velocity of 1580 fps and extends to a depth of approximately 30 ft. The second layer has a velocity of 4300 fps and ranges in depth between 66 and 80 ft where the deepest layer (bedrock) having a velocity of 10,100 fps is detected. It is noted that the forward traverse indicates an anomalous zone occurring between a distance of 240 and 360 ft relative to the forward shot point. This may be caused by localized domin$_{b}$ of the bedrock surface or by a subsurface feature having a greater velocity than the surrounding material. Seismic line R-5 (Figure 32) indicates an unequal number of layers between the forward and reverse traverses. The forward traverse indicates two velocity zones. The first zone has a velocity of 2220 fps and extends to a depth of 46 ft where the second zone, bedrock, with an apparent velocity of 7500 fps is encountered. The reverse traverse indicates three velocity layers. The first layer with a velocity of 880 fps extends to a depth of 10 ft where the second layer is encountered with a 2010-fps velocity. It appears that layer one of the forward traverse corresponds with layer two of the reverse traverse and that the first layer of the reverse traverse thins out towards the southwest. The bedrock under the

northeast shotpoint, with an apparent velocity of 9380 fps, is detected at a depth of 38 ft. The true velocity of the bedrock for line R-5 is 8335 fps. Figure 33 presents the TD information gathered from the conduct of line R-6. Two velocity layers were determined as a result of the testing. The first layer has a velocity of 1950 fps and has a thickness ranging between 33 and 36 ft and is underlain by a second layer, bedrock, which has a true velocity of 7310 fps. An anomalous zone is indicated by the data at distances ranging between 180 and 350 ft from the southwestern shotpoint. Referring to Figure 34, line R-7, two velocity layers are indicated. The first layer has an average velocity of 2100 fps and extends to depths ranging between 50 and 52 ft and is underlain by bedrock with a true velocity of 9610 fps. An anomalous feature extending between a distance of 190 and 240 ft, relative to the northern shotpoint, is indicated by the data. Figure 35 presents a summary of the seismic refraction results. Figure 36 presents a contour map of the elevation of the top of rock. The top of rock elevations were obtained by estimating the elevation of the refraction survey shot points and subtracting the calculated overburden thickness. This gave a total of 14 depth data points (one data point under each shot point) to be used as input for a computer contouring program. The possibility of a sinkhole centered on approximate coordinates (500,325) is evident.

PART VI: CONCLUSIONS

19. Two geophysical methods were employed at HWMS-16 in an attempt to delineate zones having anomalous terrain conductivity conditions and to determine the depth to rock. With regard to the surveys performed during the period 26 February through 6 March 1987, the following conclusions are made:

a. The EM surveys delineated several zones having anomalous conductivity values. The method was successful in determining the locations of buried landfill cells. Also, it was determined that cell #4, used for burying hazardous waste material exhibited the highest conductivity values.

b. Two possible contaminant plumes were indicated by an EM survey conducted around the perimeter of the site.

c. Although the site was heterogeneous in character, the seismic refraction lines were successful in determining the depth to top of rock and also in determining the P-wave velocities for the various layers at the site. A possible sinkhole centered on approximate coordinate (500,325) was detected with the seismic refraction technique.

REFERENCES

Aycock, M. J., Jr. 1987 (Aug). "Feasibility Study for Hazardous Waste Management Sites 4, 5, 7, and 16, Radford Army Ammunition Plant, VA," Preliminary Draft Report, Hilton Systems, Inc. Vicksburg, Miss.

Butler, D. K. 1986. "Military Hydrology; Report 10: Assessment and Field Examples of Continuous Wave Electromagnetic Surveying for Ground Water," Miscellaneous Paper EL-79-6, U.S. Army Engineer Waterways Experiment Station, Vicksburg, Miss.

Department of the Army 1979. Geophysical Exploration, Engineer Manual EM 1110-1-1802, Office of the Chief of Engineers, Washington, D.C.

McNeil, J. D. 1980. "Electromagnetic Terrain Conductivity Measurement at Low Induction Numbers," Technical Note TN-6, Geonics Limited, Mississauga, Ontario, Canada.

McNeil, J. D. 1985. "EM34-3 Measurements at Two Inter-Coil Spacings to Reduce Sensitivity to Near-Surface Material," Technical Note TN-19, Geonics Limited, Mississauga, Ontario, Canada.

Porter, R. S., Jr. and Sipher, D. J. 1984 (Nov). "Groundwater Monitoring Well Installation, Horseshoe Area, Radford Army Ammunition Plant, VA," Letter Report, Froehling and Robertson, Inc., Roanoke, VA.

Telford, W. M., Geldhart, L. P., Sheriff, R. E., and Keys, D. A. 1973. Applied Geophysics, Cambridge University Press, New York.

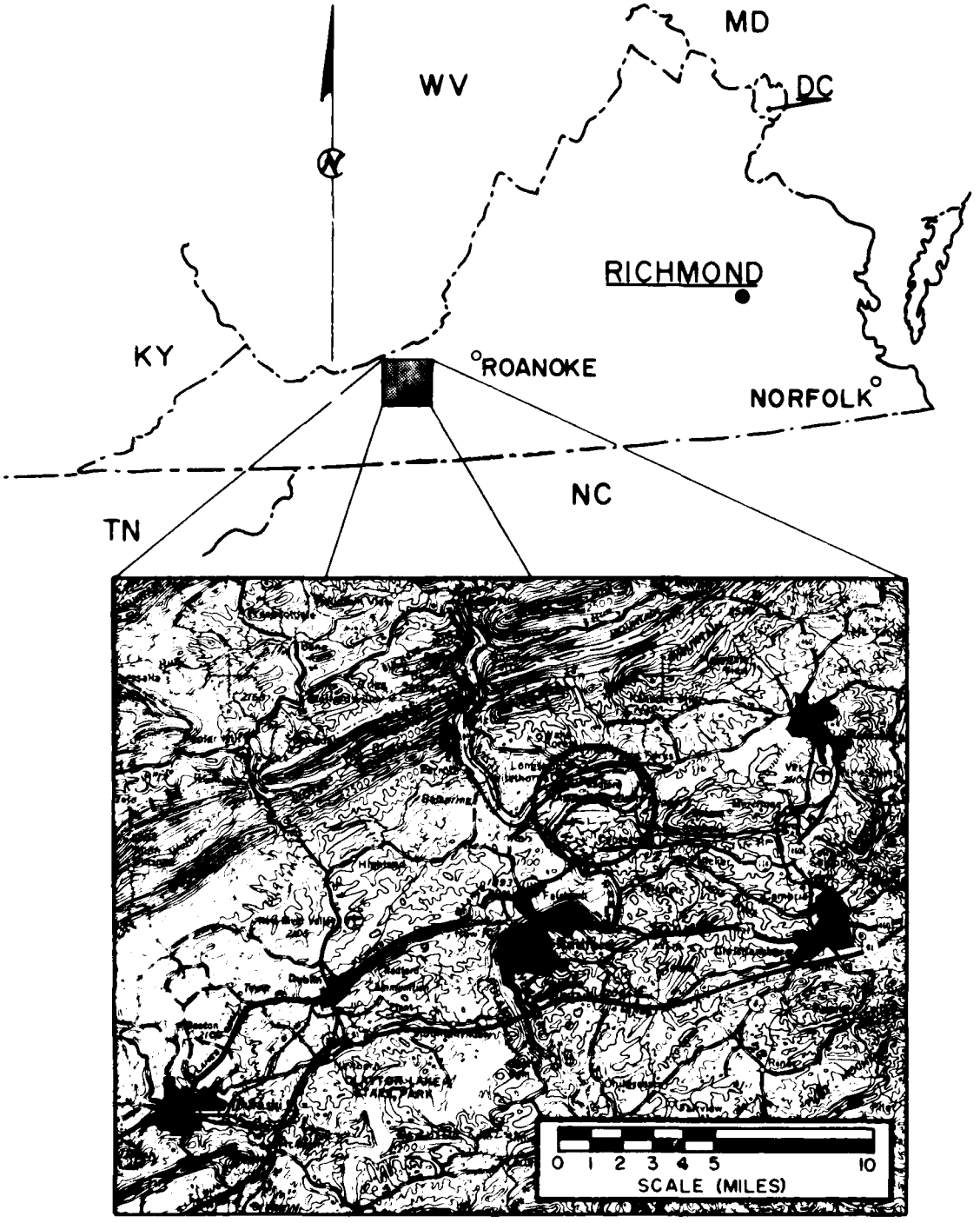

Figure 1. Vicinity map

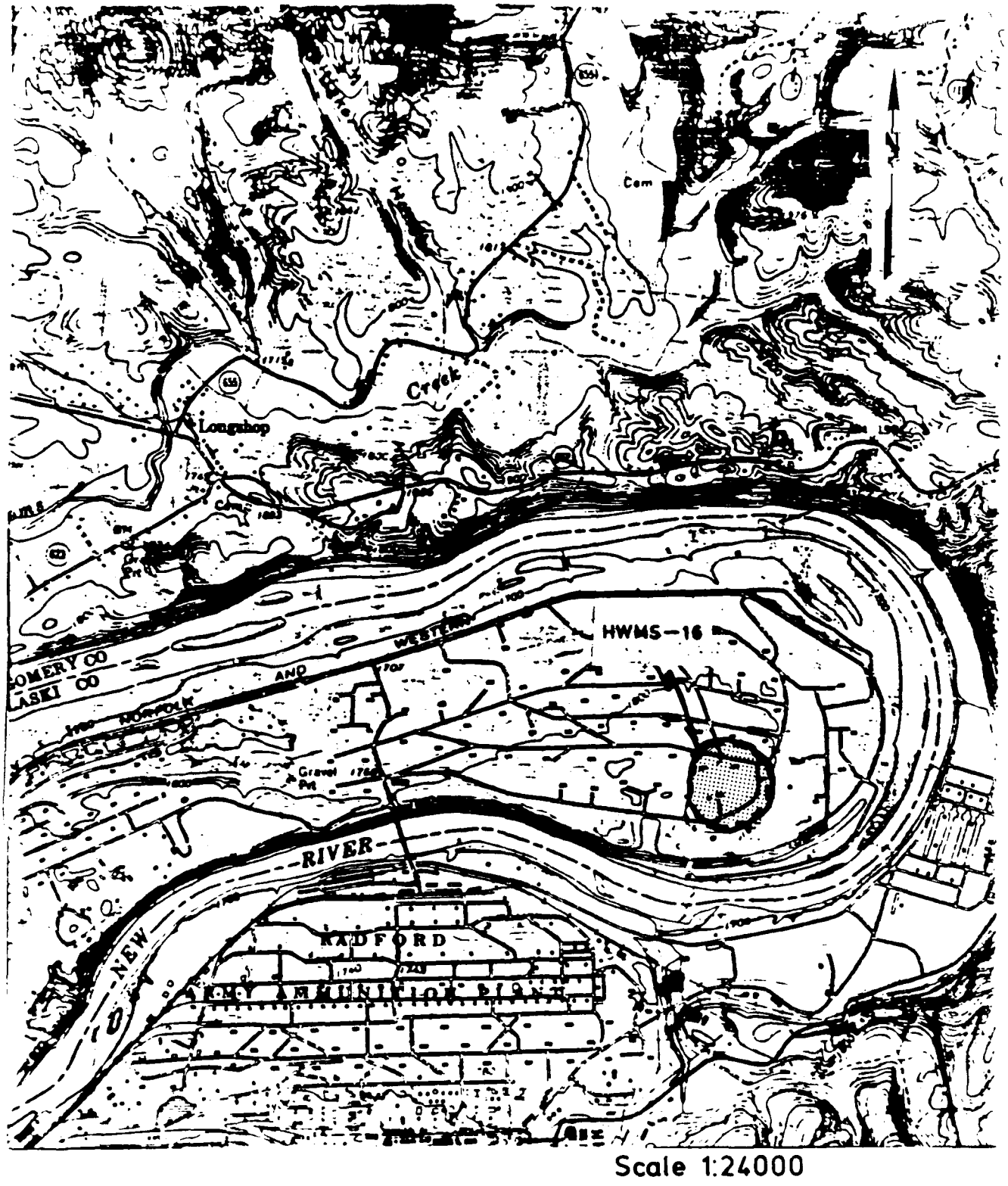

Figure 2. Site map showing location of Hazardous Waste Management Site 16

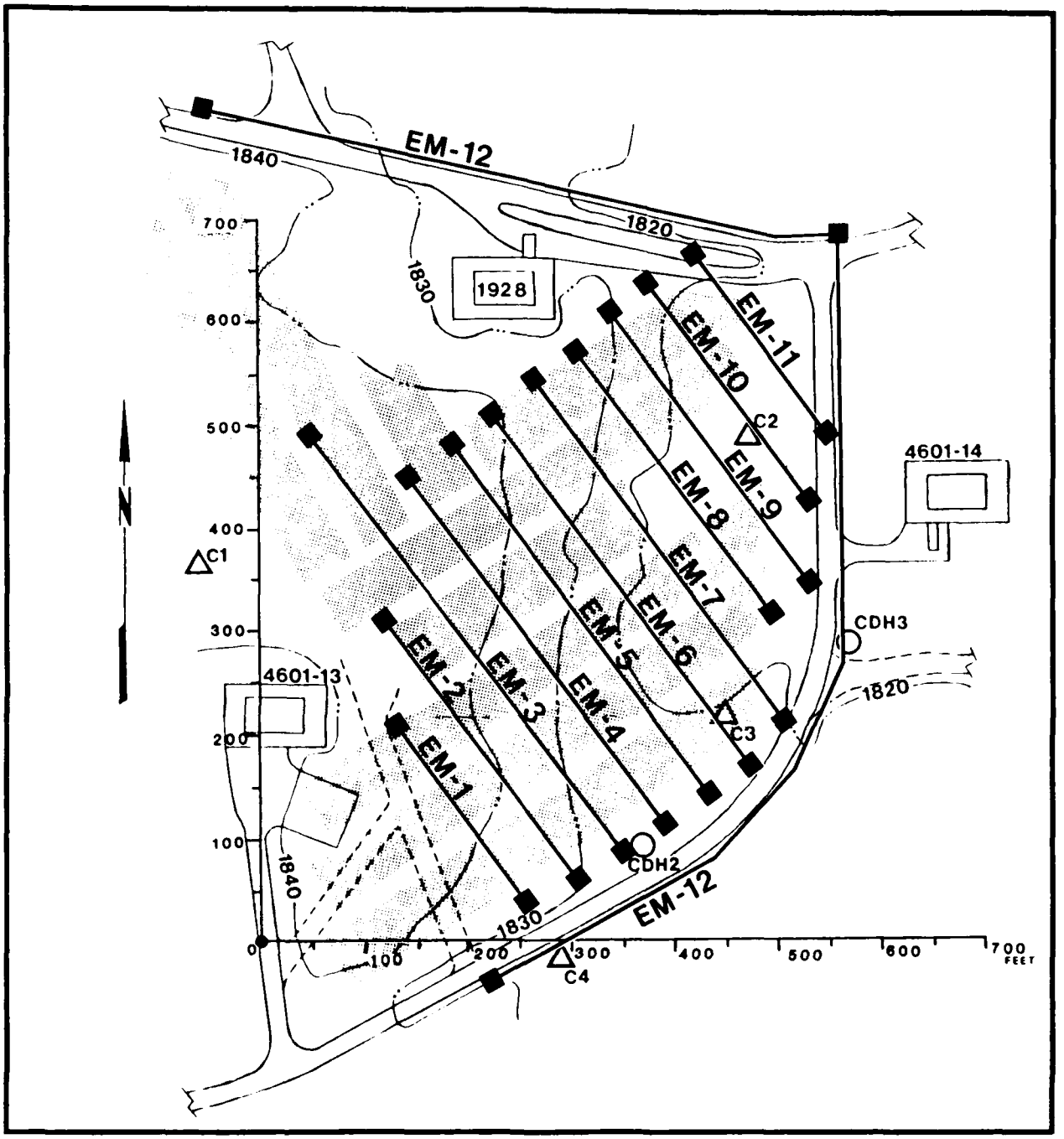

△C3 ○CDH2 **Well Positions**

EM-8 **EM Profile Line**

Figure 3. Location and orientation of EM lines

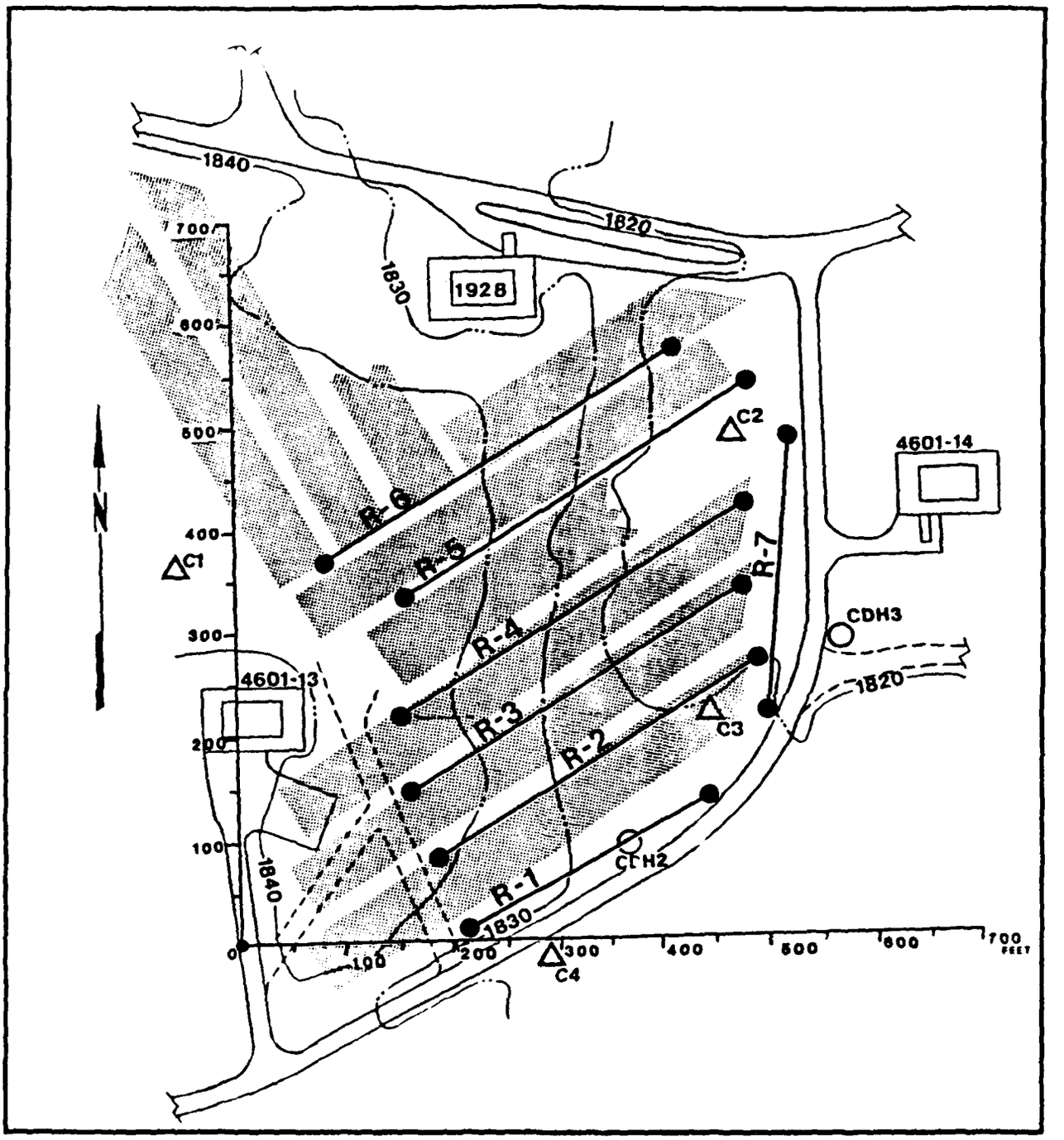

△C2 ○CDH3 **Well Positions**

●—R-3—● **Refraction Profile Line**

Figure 4. Location and orientation of seismic refraction lines

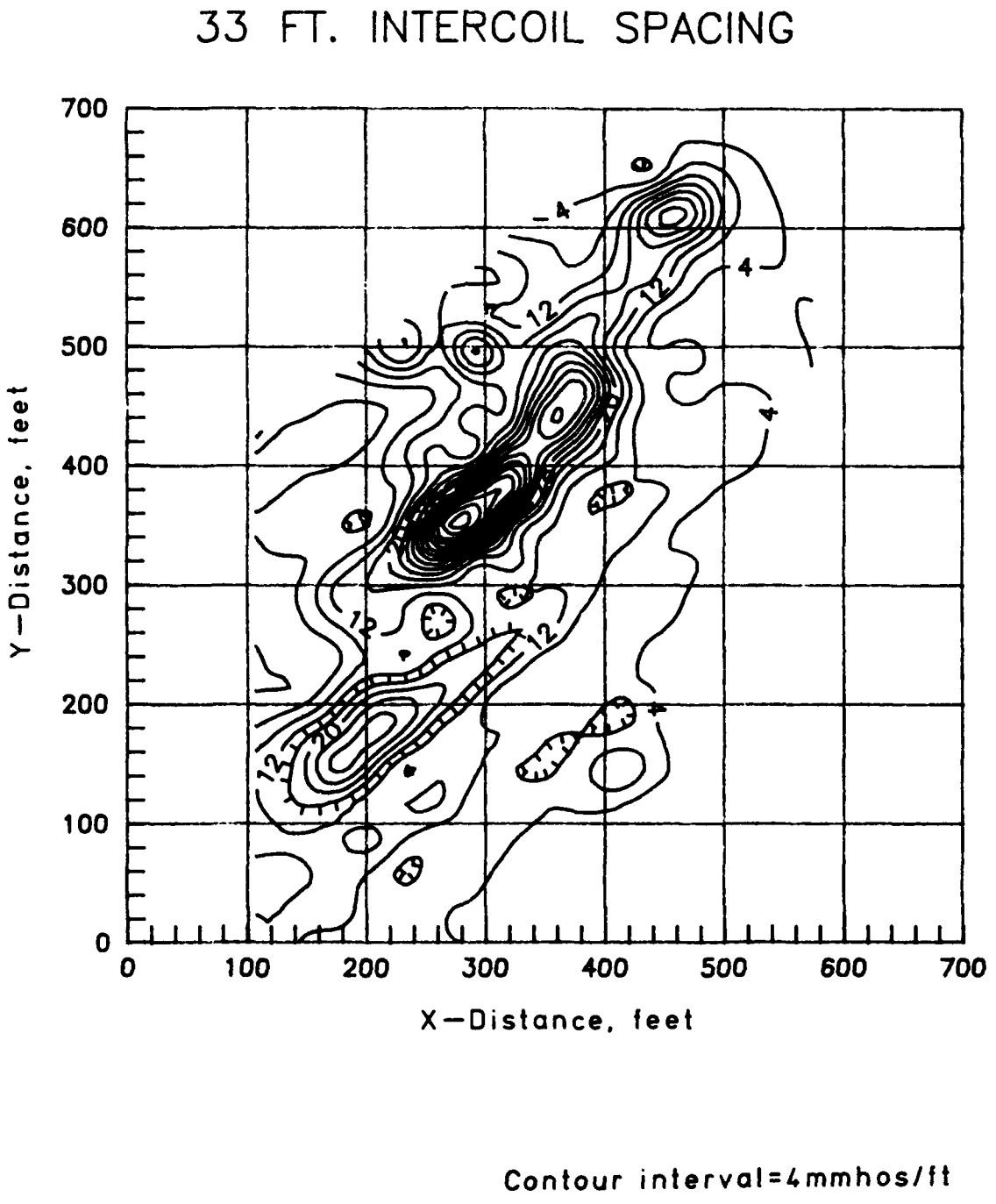

Figure 5. 2-D EM data, 33 ft intercoil spacing, perpendicular orientation

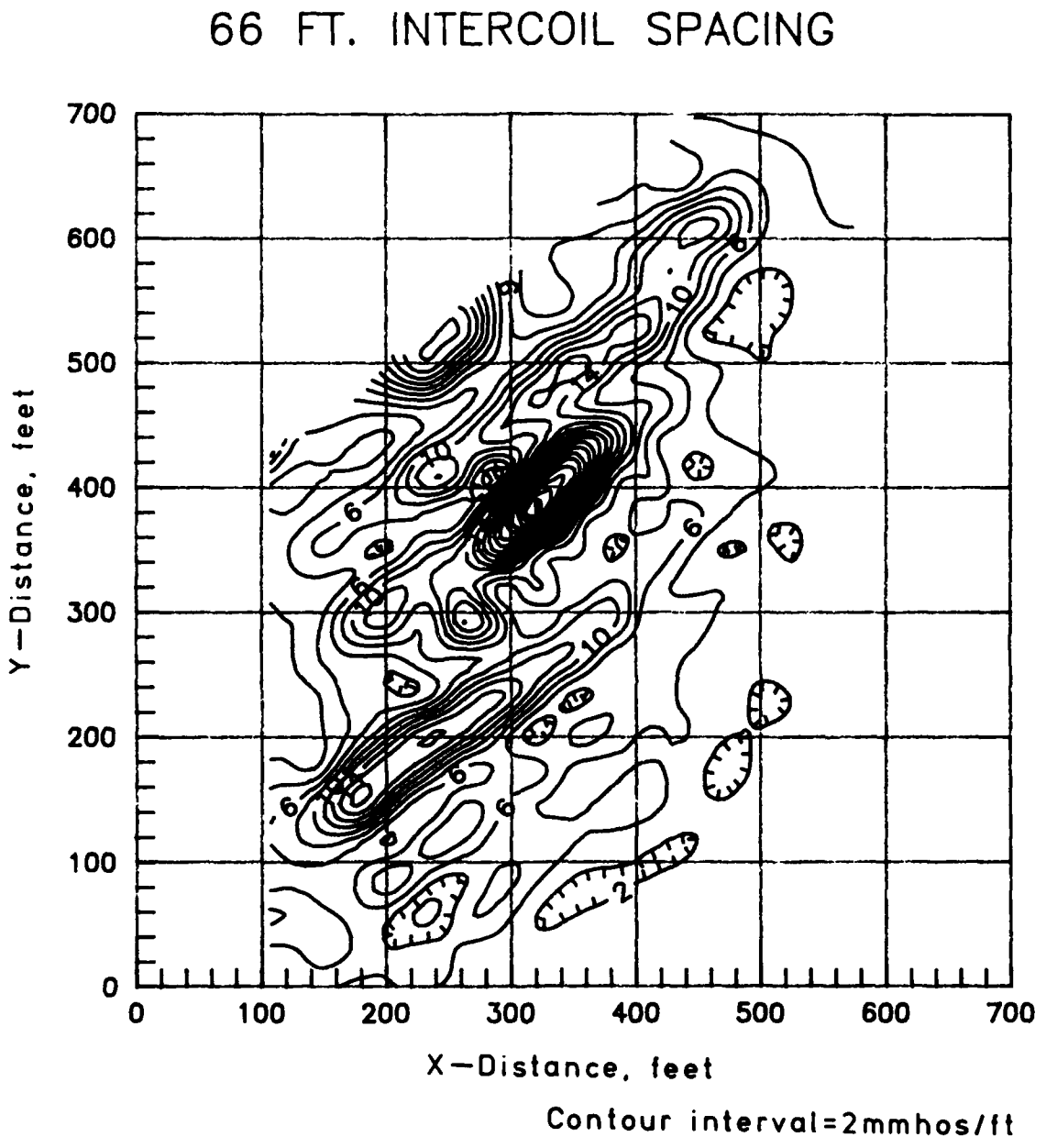

Figure 6. 2-D EM data, 66 ft intercoil spacing, perpendicular orientation

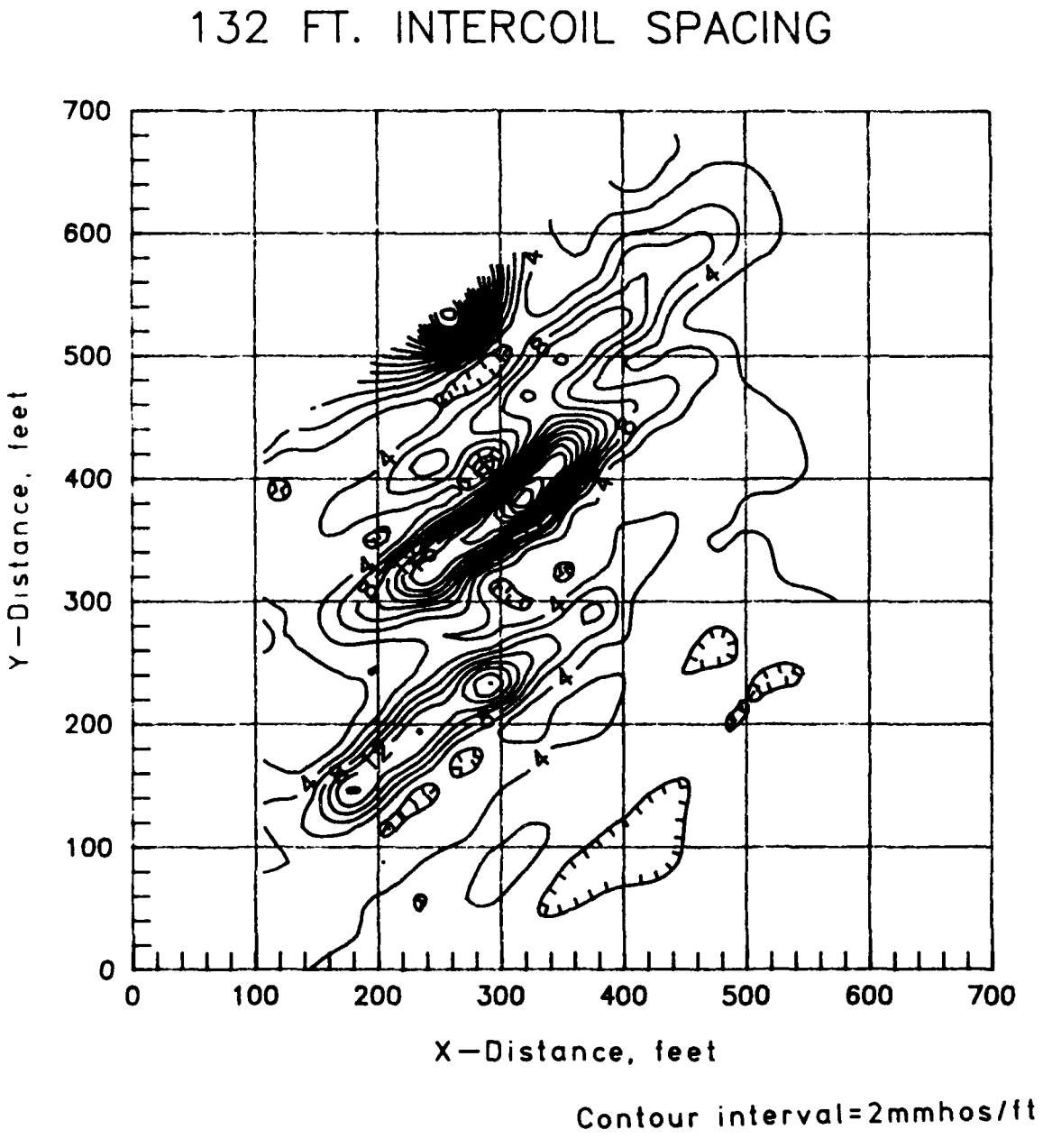

Figure 7. 2-D EM data, 132 ft intercoil spacing, perpendicular orientation

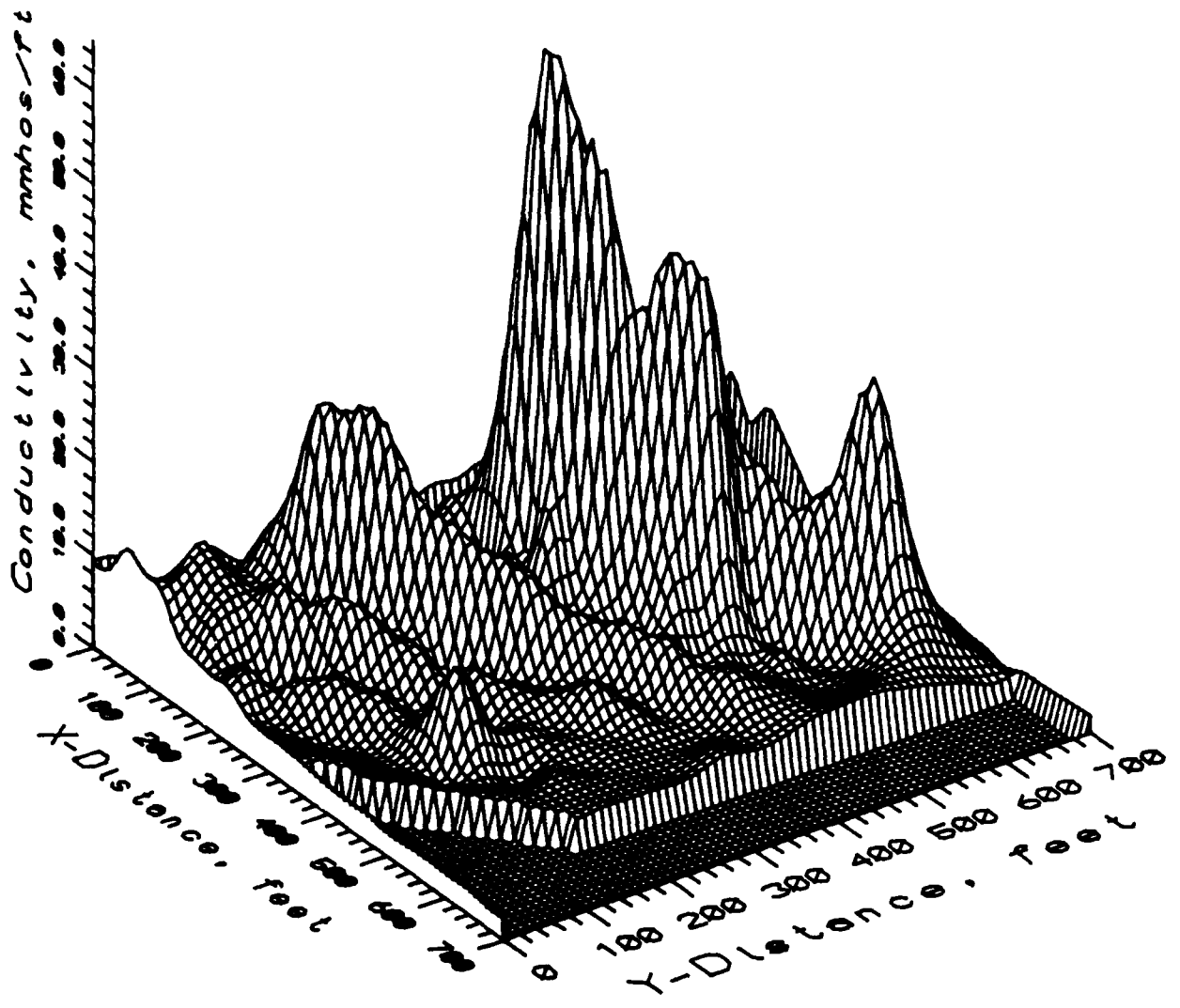

33 FT. INTERCOIL SPACING

Figure 8. 3-D EM data, 33 ft intercoil spacing, perpendicular orientation

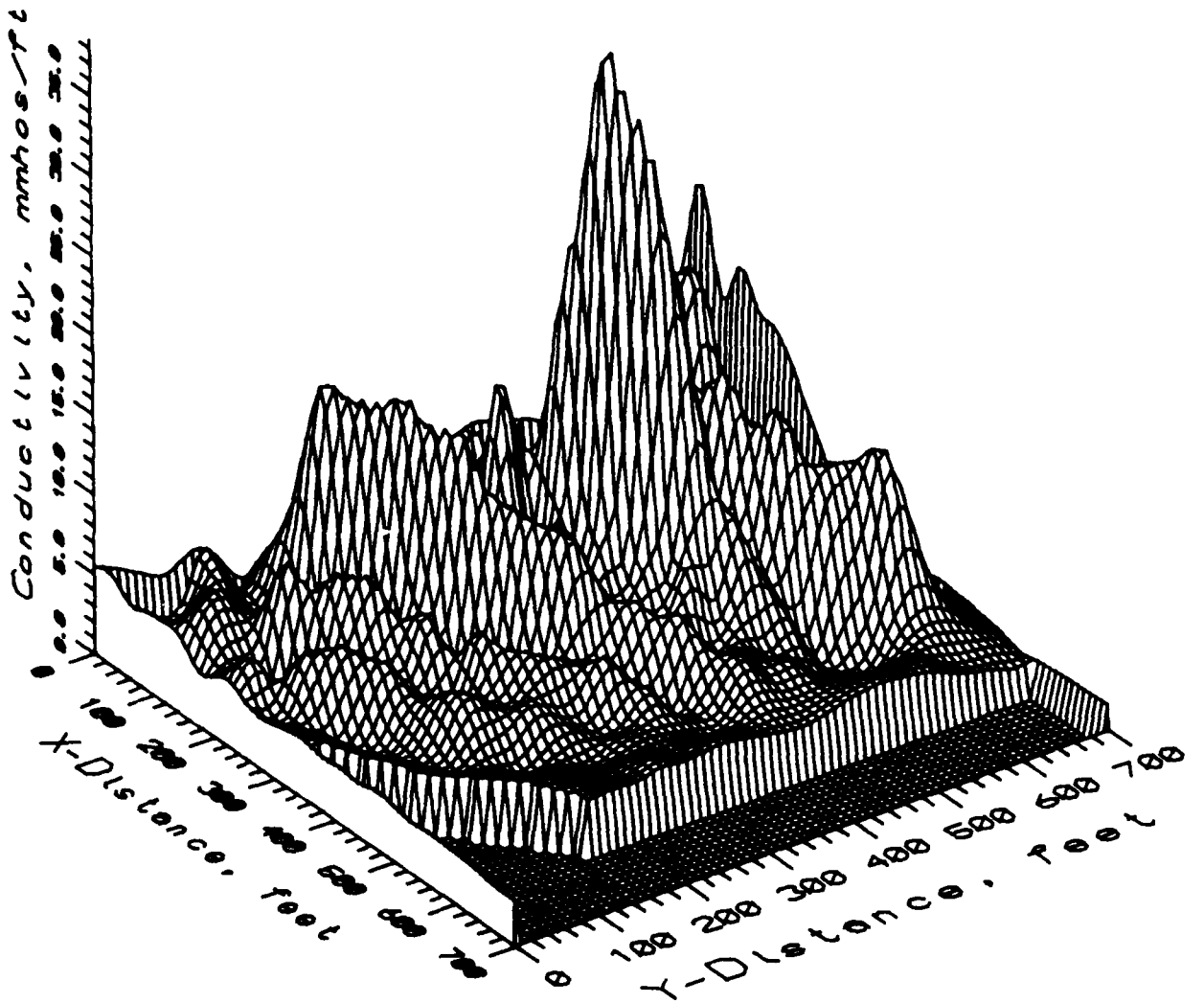

66 FT. INTERCOIL SPACING

Figure 9. 3-D EM data, 66 ft intercoil spacing, perpendicular orientation

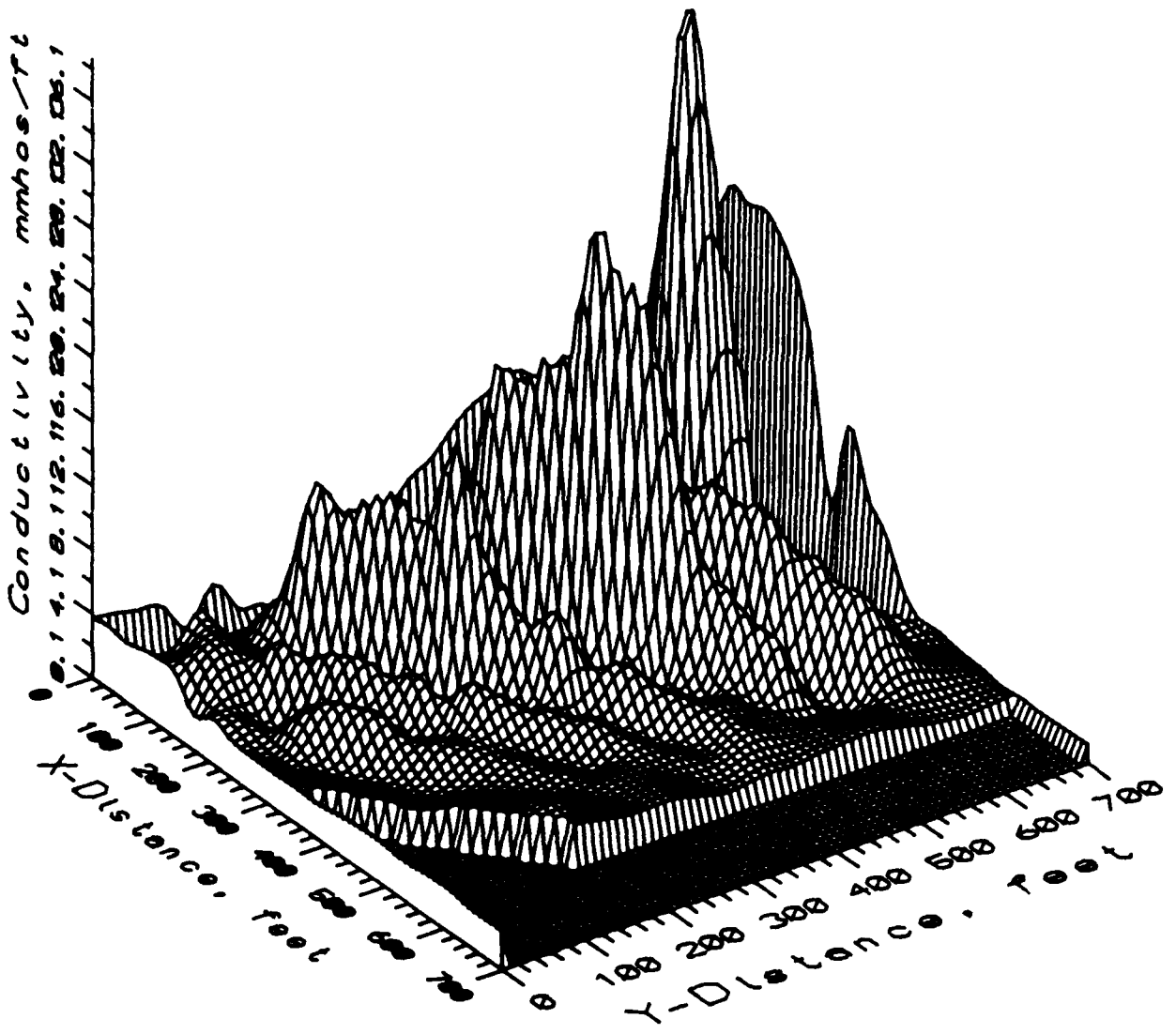

132 FT. INTERCOIL SPACING

Figure 10. 3-D EM data, 132 ft intercoil spacing, perpendicular orientation

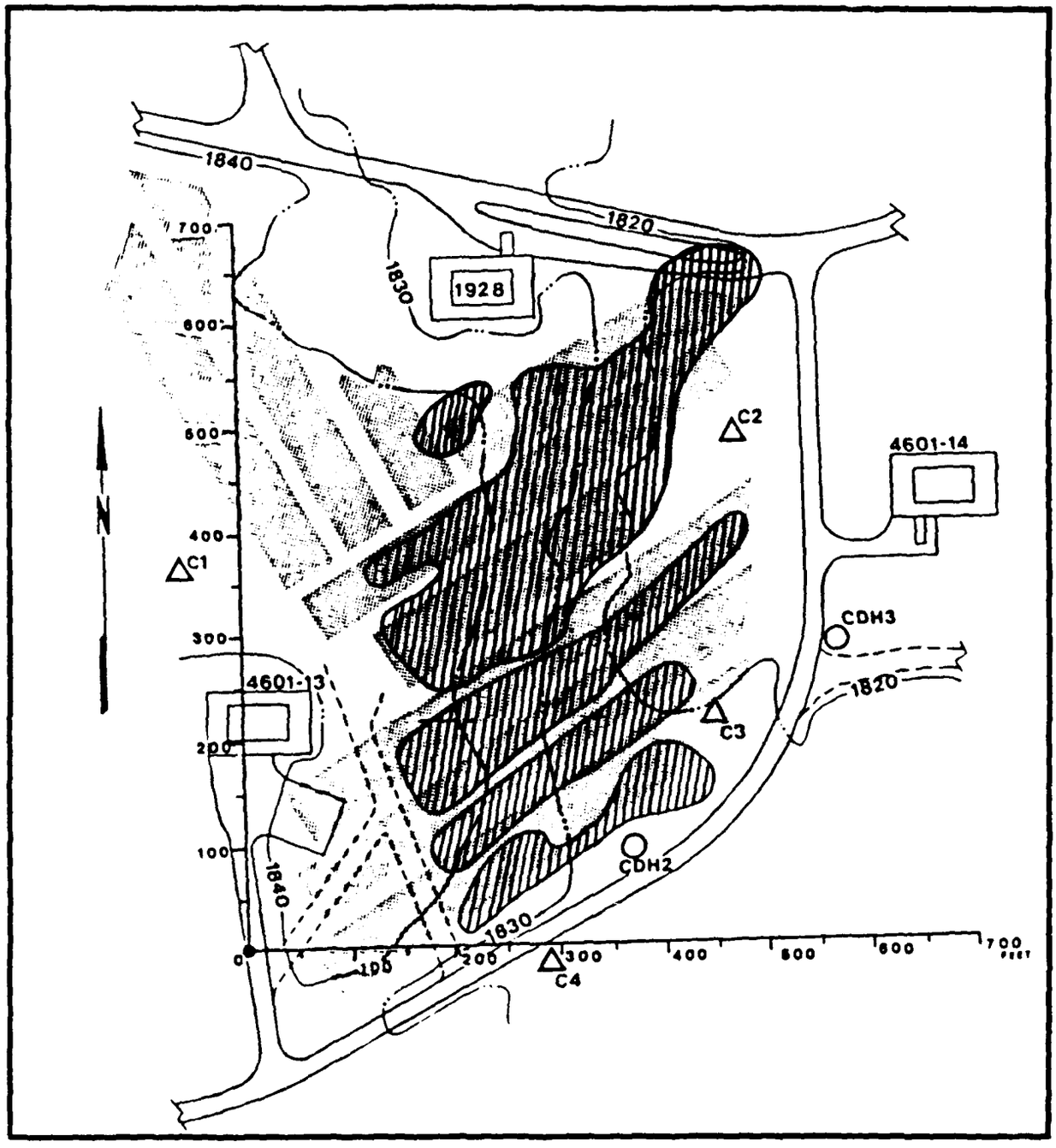

CDH3 C4 **Well Positions**

Actual Location of Landfill Cells

Interpreted Location of Landfill Cells -- (33 feet)

Figure 11. Interpreted location of landfill cells, 33 ft intercoil spacing, perpendicular orientation

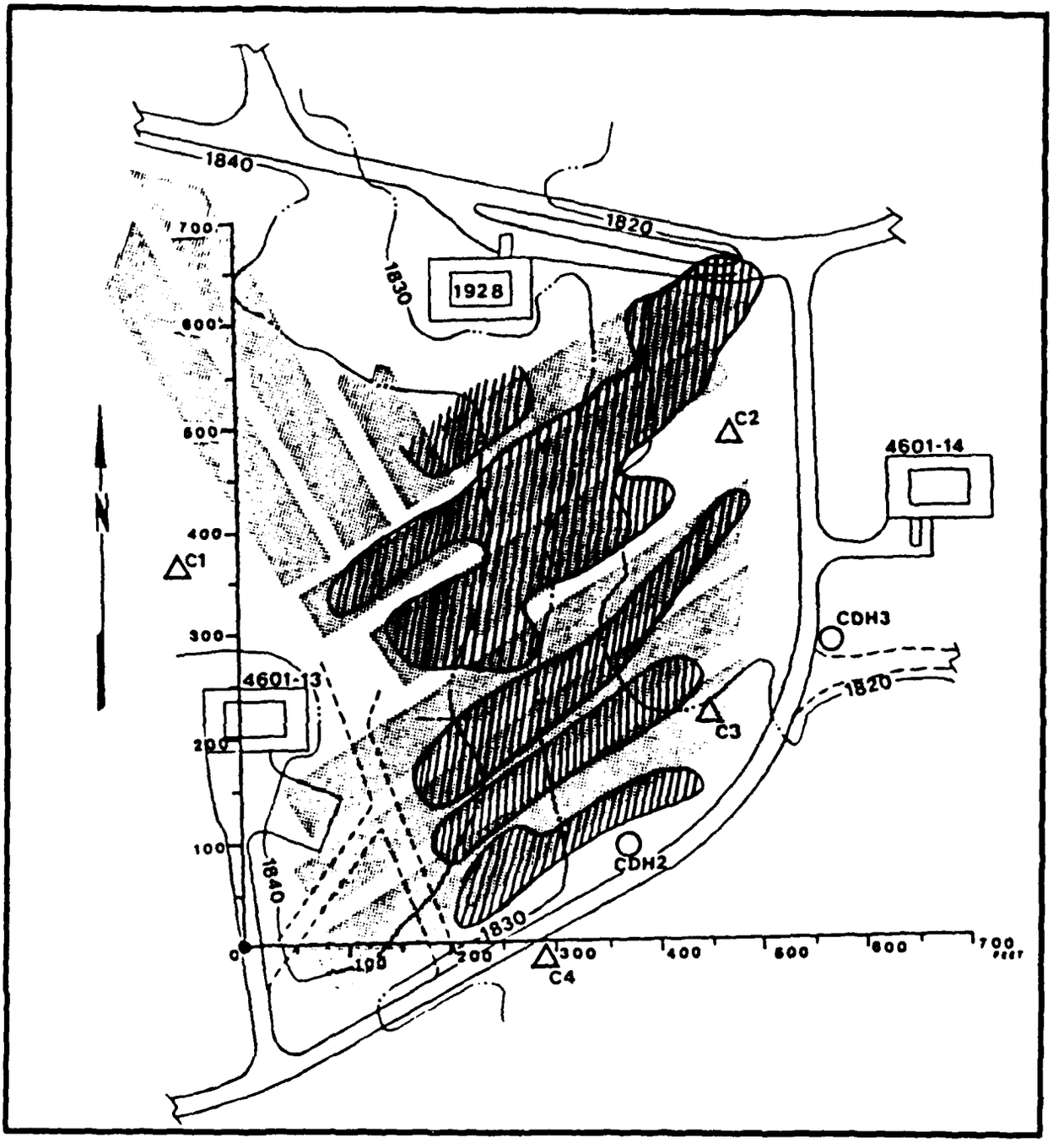

CDH3 C4 **Well Positions**

Actual Location of Landfill Cells

Interpreted Location of Landfill Cells -- (66 feet)

Figure 12. Interpreted location of landfill cells, 66 ft intercoil spacing, perpendicular orientation

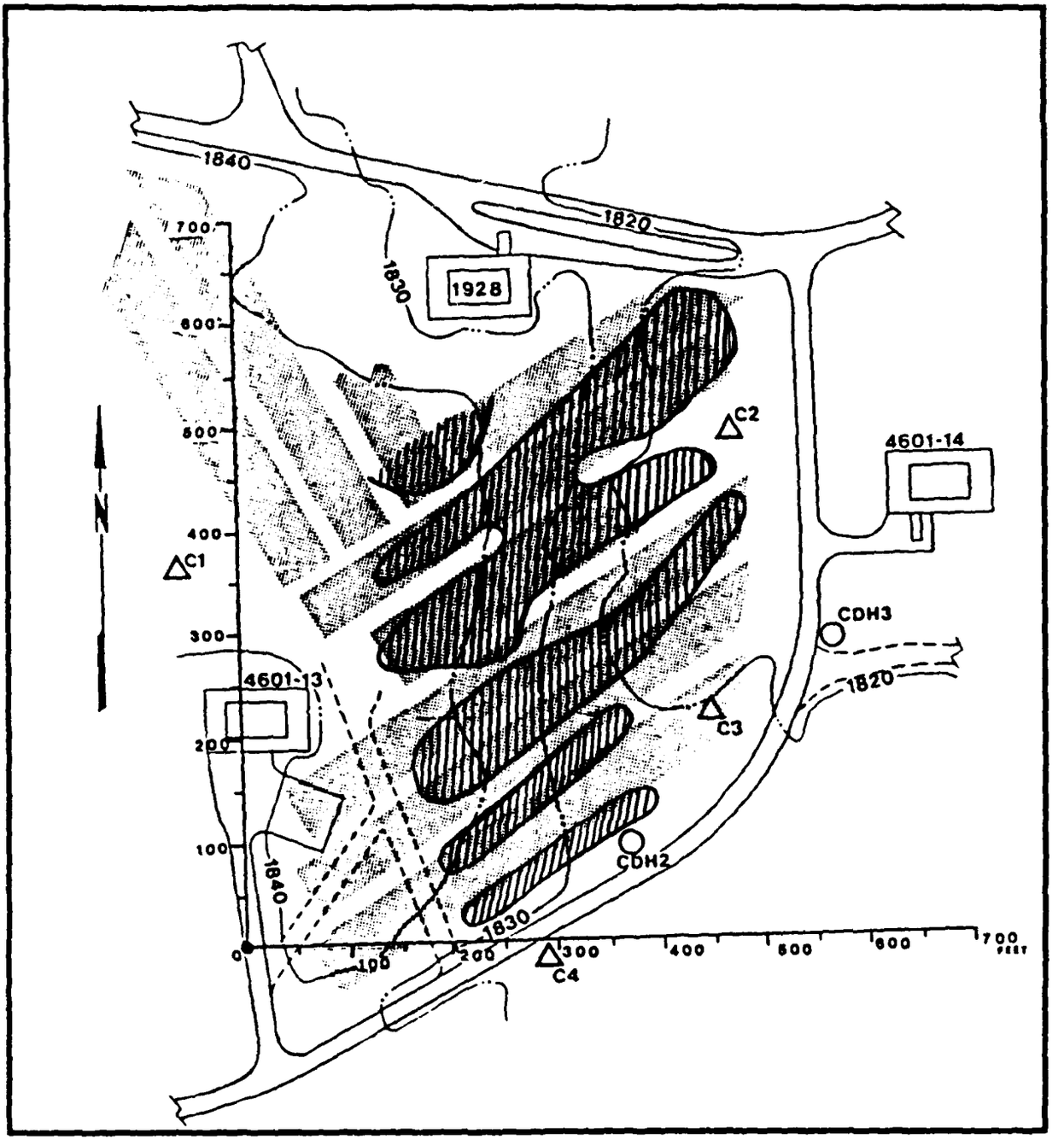

CDH3 C4 **Well Positions**

Actual Location of Landfill Cells

Interpreted Location of Landfill Cells -- [132 feet]

Figure 13. Interpreted location of landfill cells, 132 ft intercoil spacing, perpendicular orientation

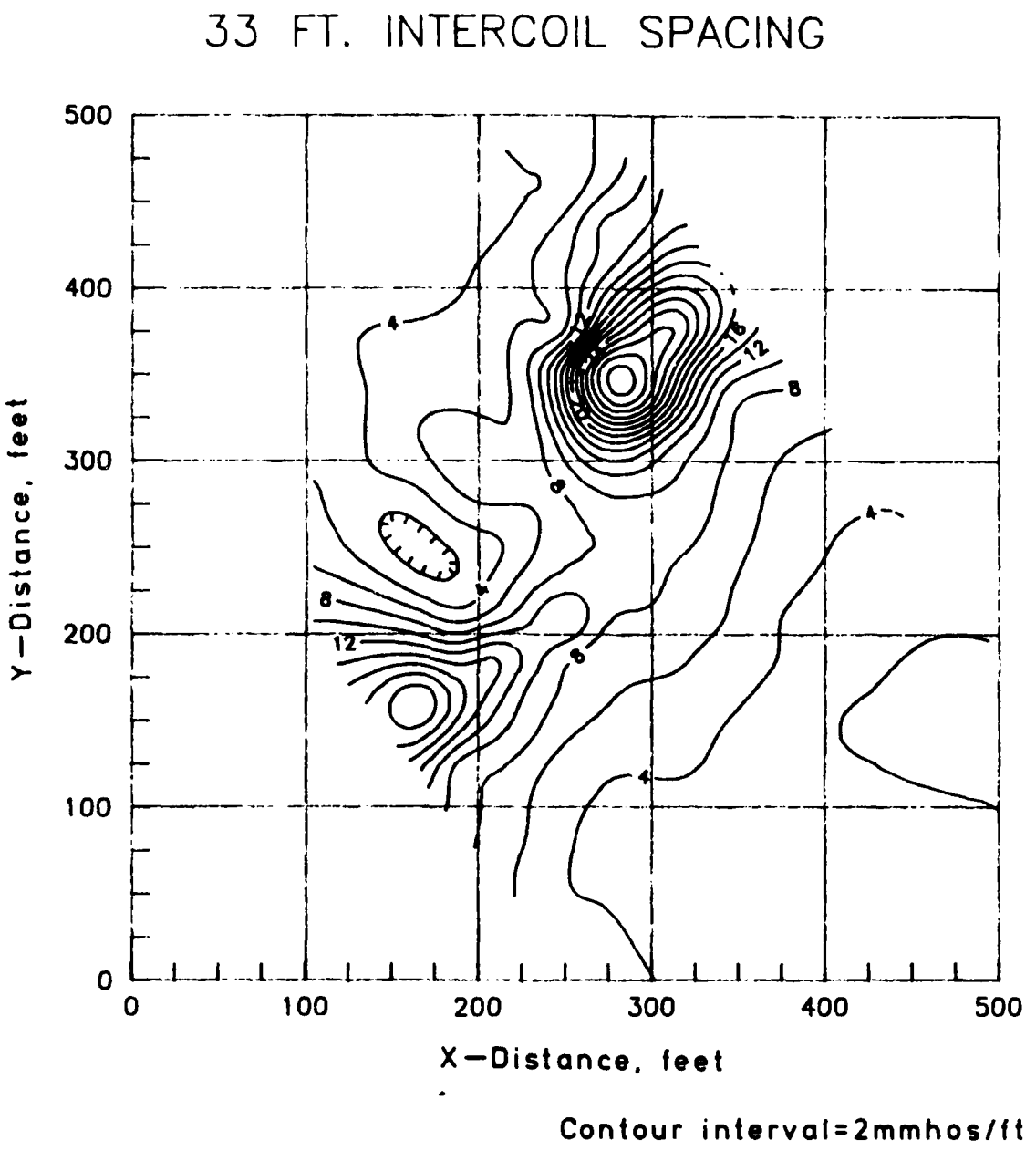

Figure 14. 2-D EM data, 33 ft intercoil spacing, parallel orientation

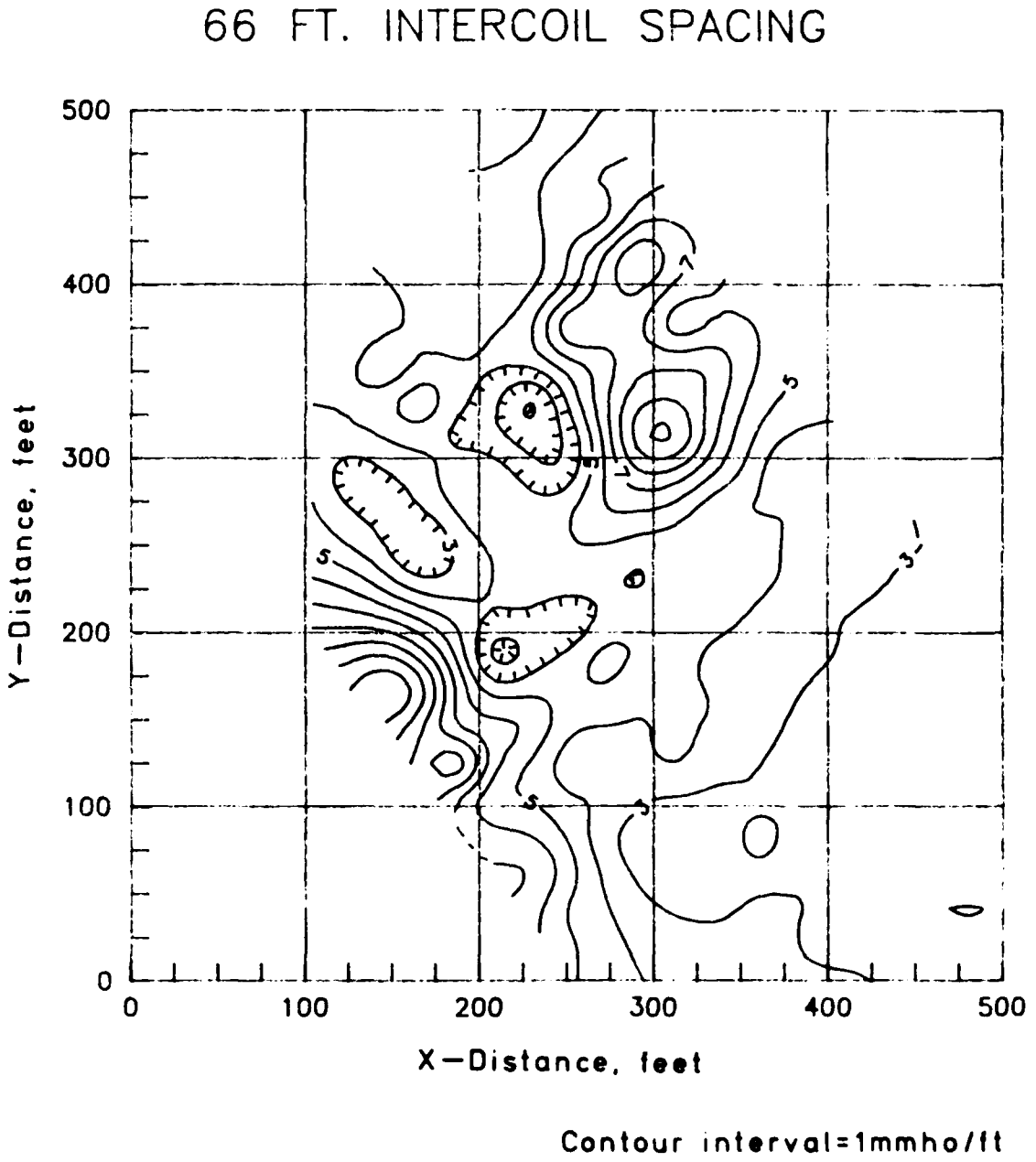

Figure 15. 2-D EM data, 66 ft intercoil spacing, parallel orientation

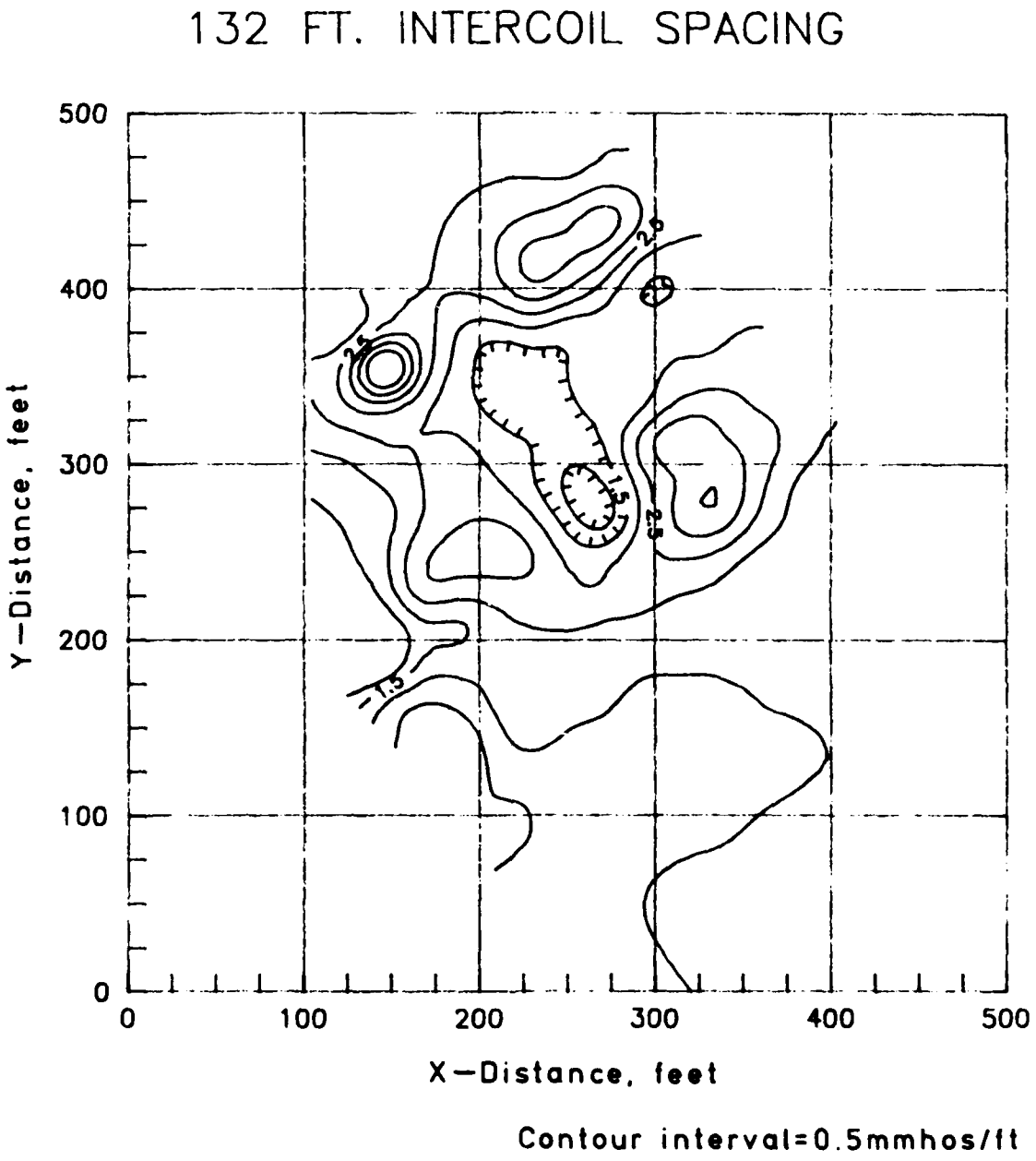

Figure 16. 2-D EM data, 132 ft intercoil spacing, parallel orientation

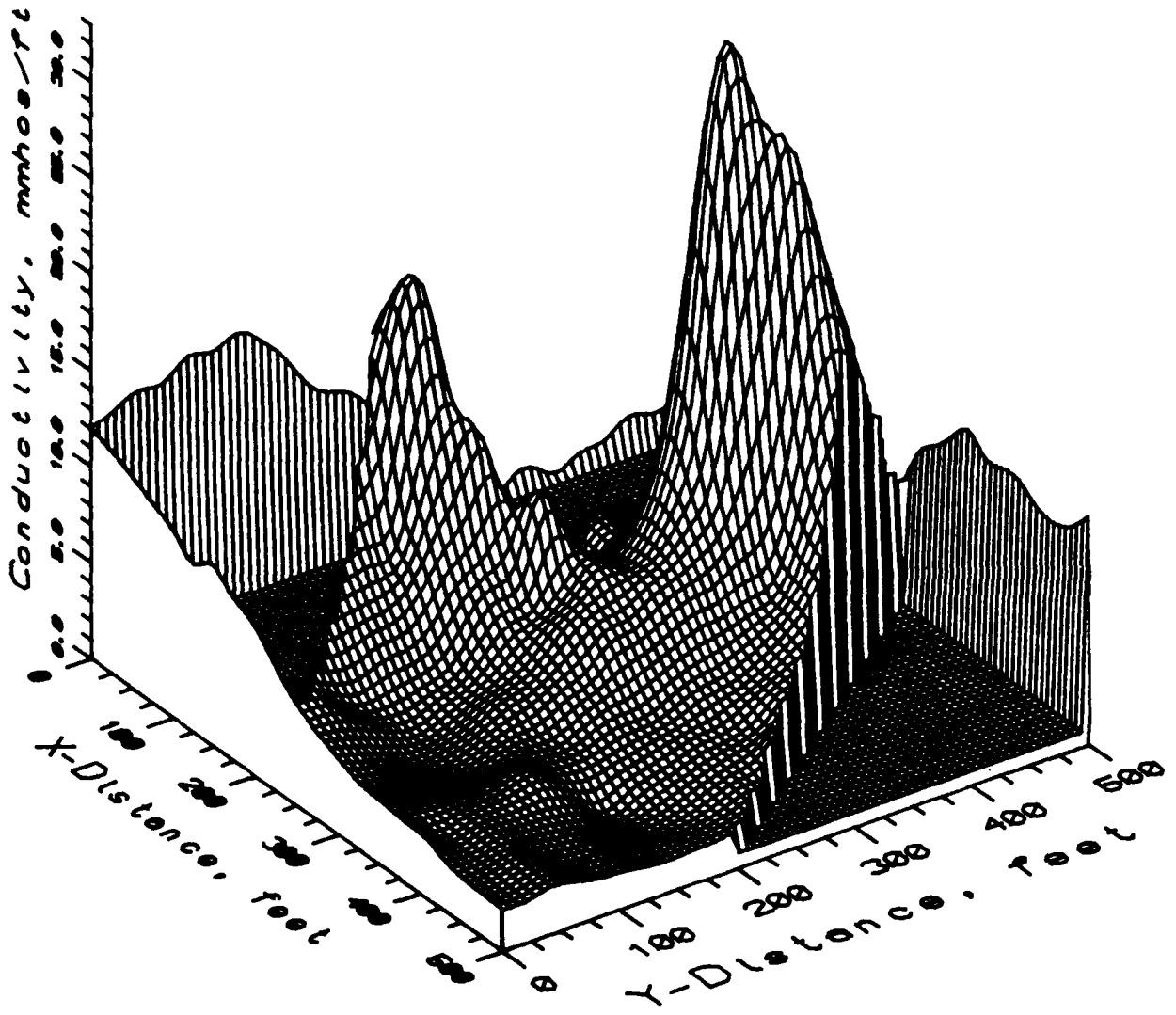

33 FT. INTERCOIL SPACING

Figure 17. 3-D EM data, 33 ft intercoil spacing, parallel orientation

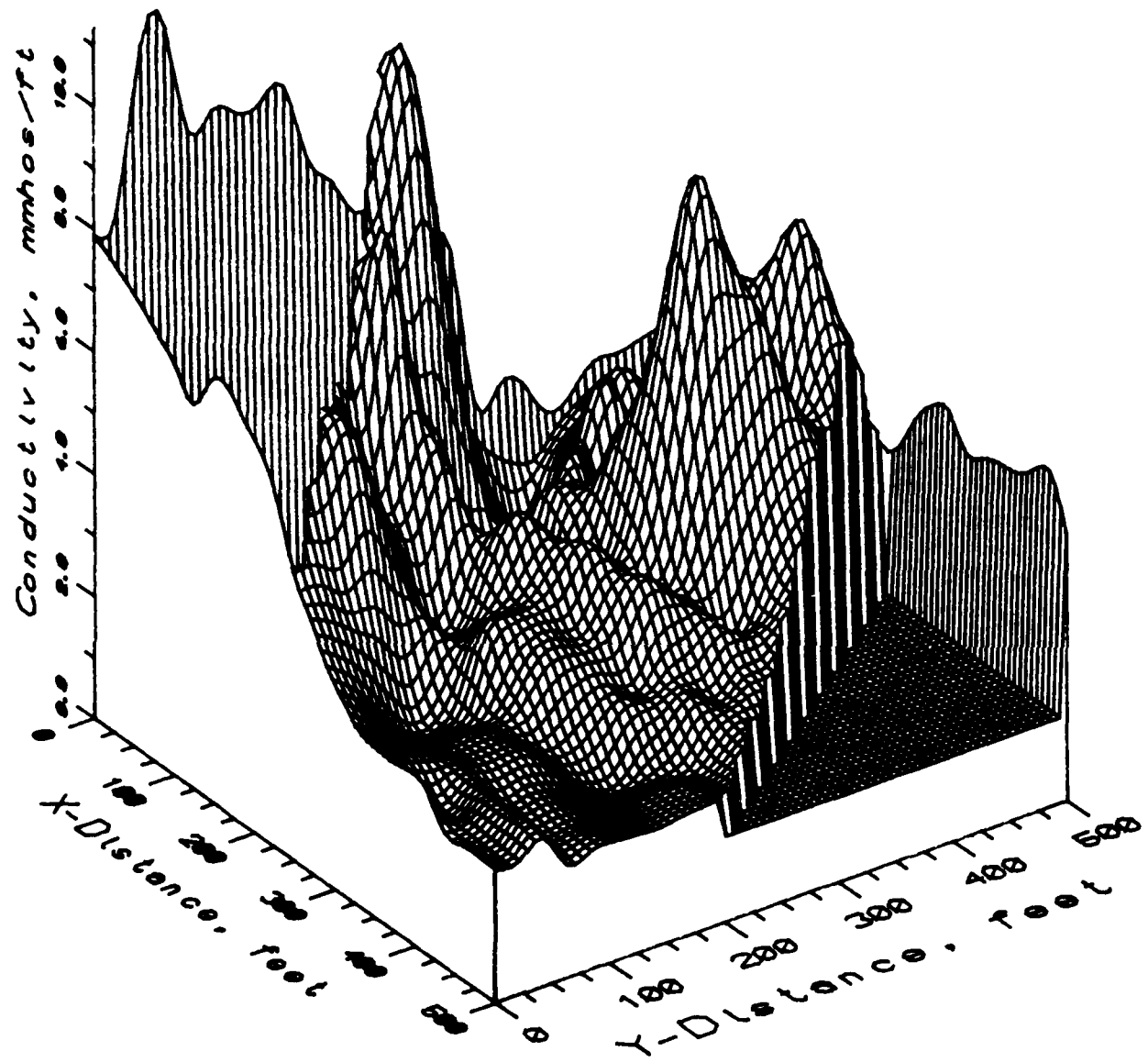

Figure 18. 3-D EM data, 66 ft intercoil spacing, parallel orientation

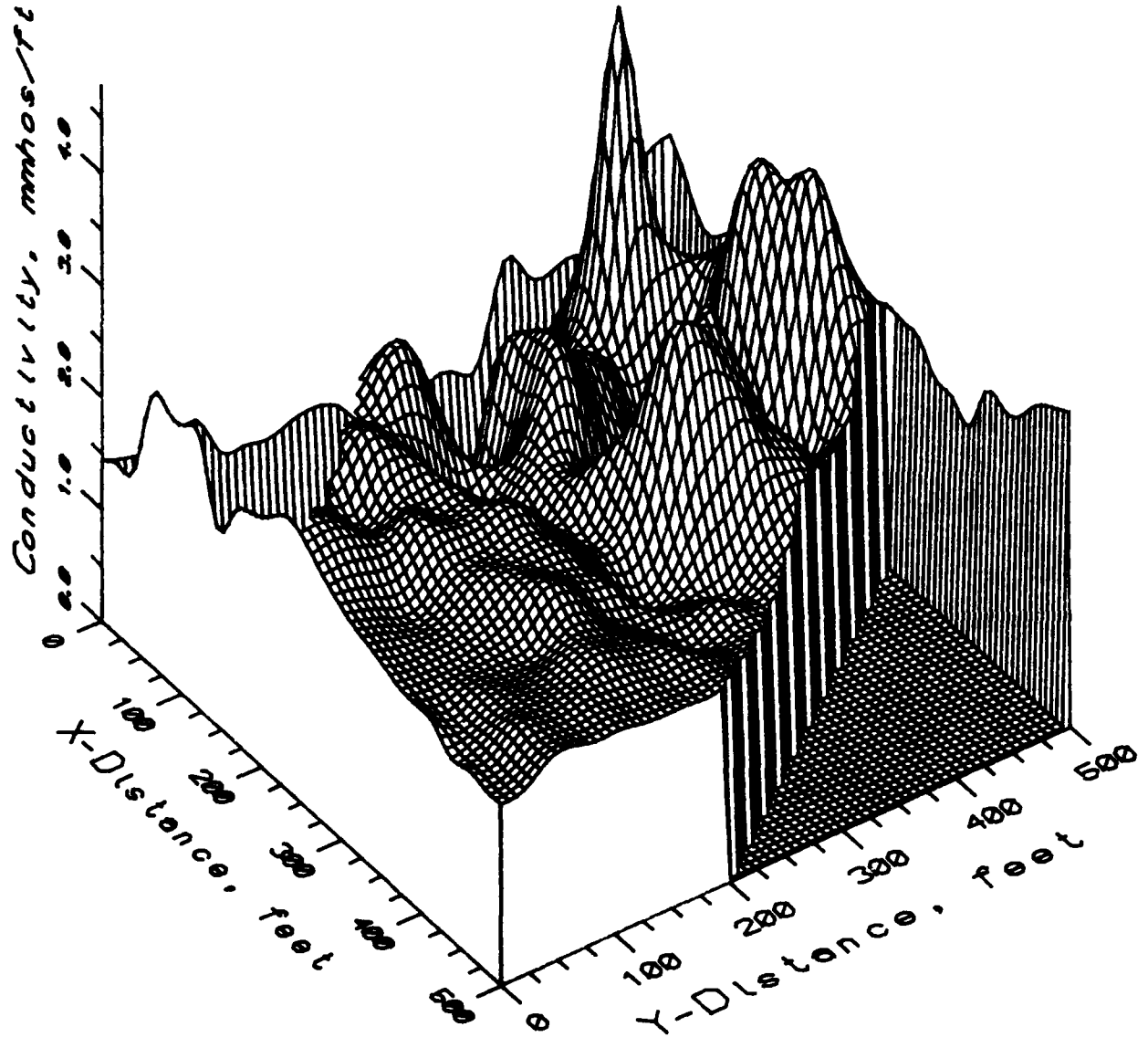

Figure 19. 3-D EM data, 132 ft intercoil spacing, parallel orientation

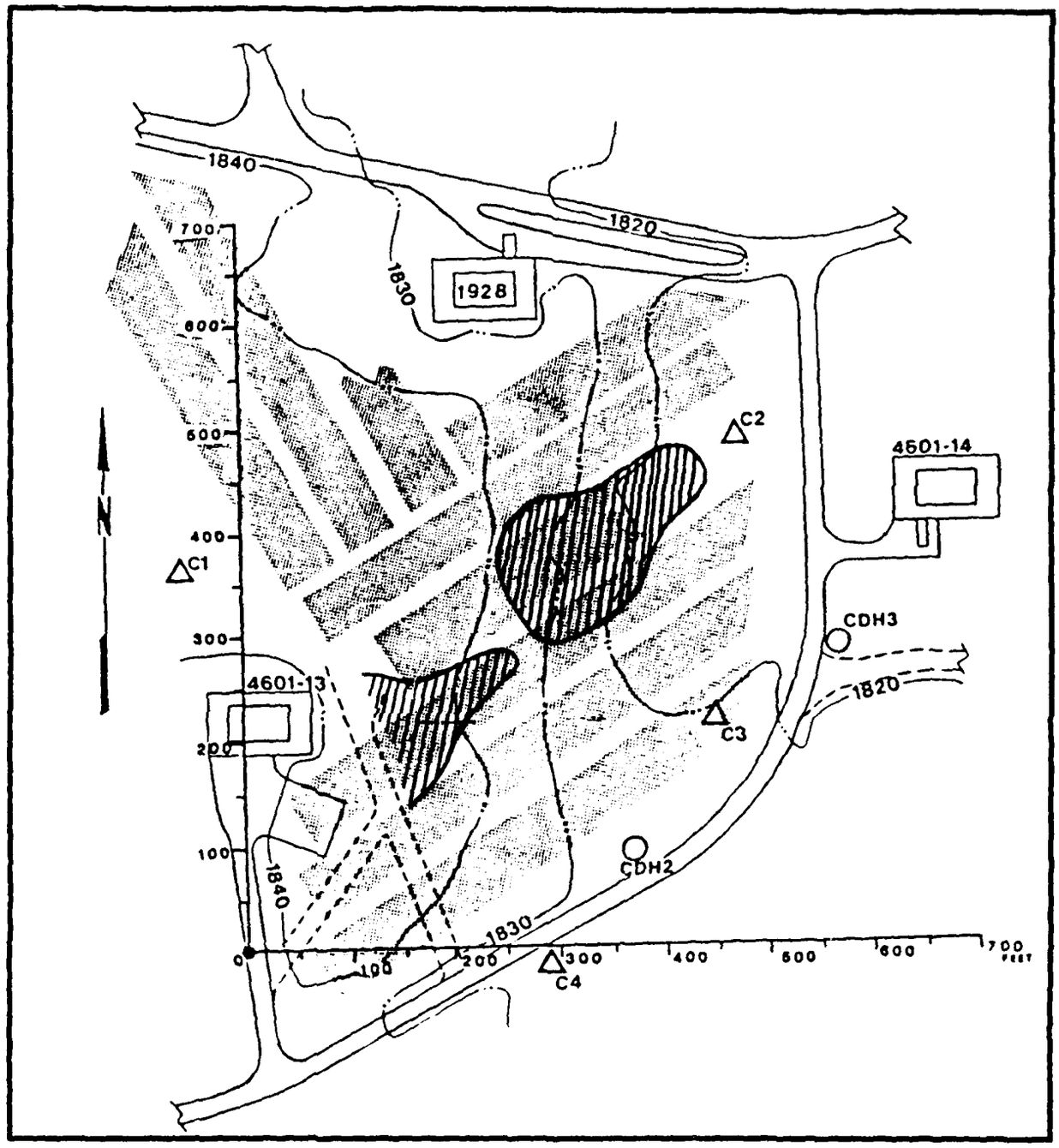

CDH3 C4 **Well Positions**

Actual Location of Landfill Cells

Interpreted Location of Landfill Cells -- (33 feet)

Figure 20. Interpreted location of landfill cells, 33 ft intercoil spacing, parallel orientation

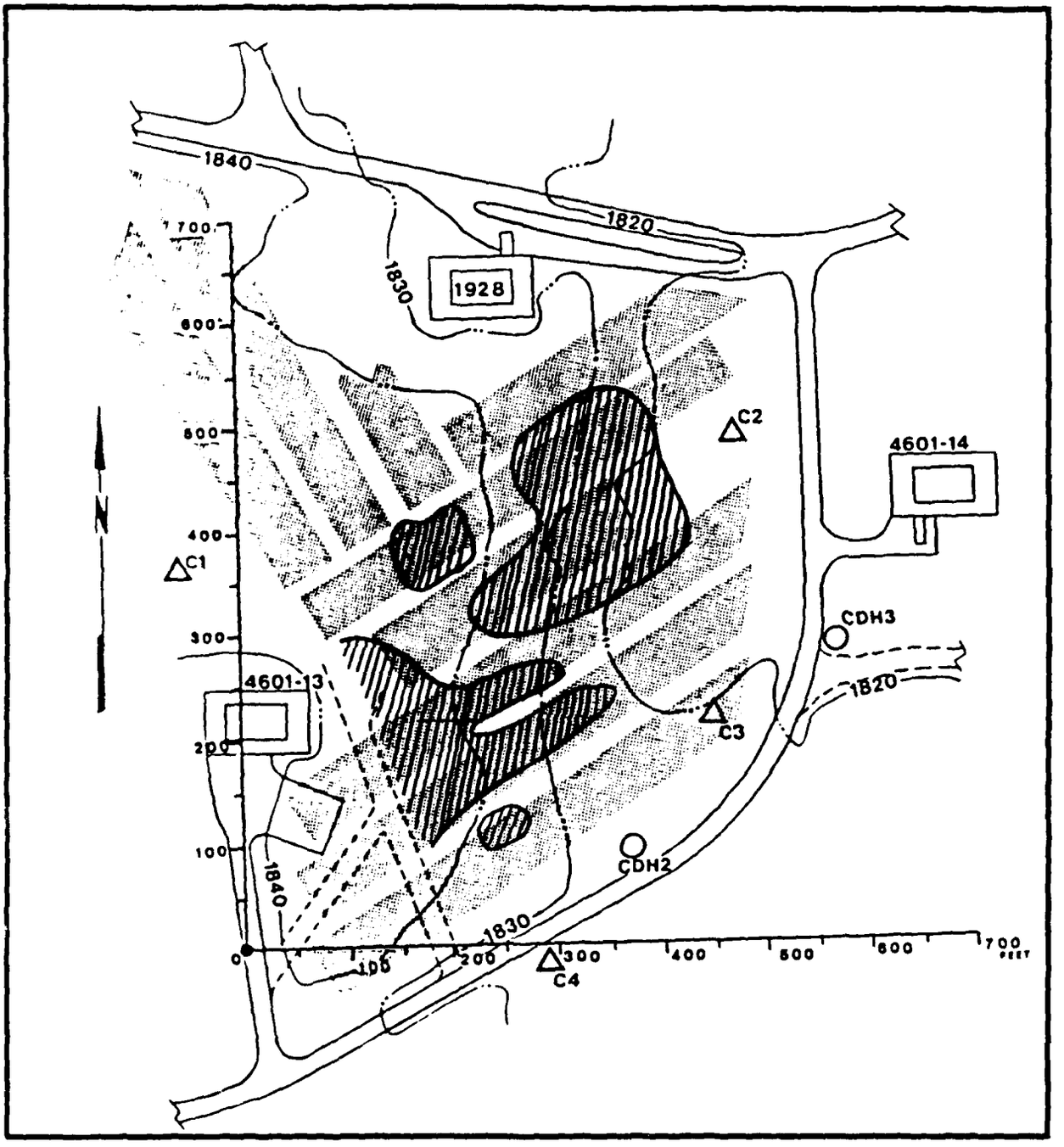

CDH3 C4 **Well Positions**

Actual Location of Landfill Cells

Interpreted Location of Landfill Cells -- (66 feet)

Figure 21. Interpreted location of landfill cells, 66 ft intercoil spacing, parallel orientation

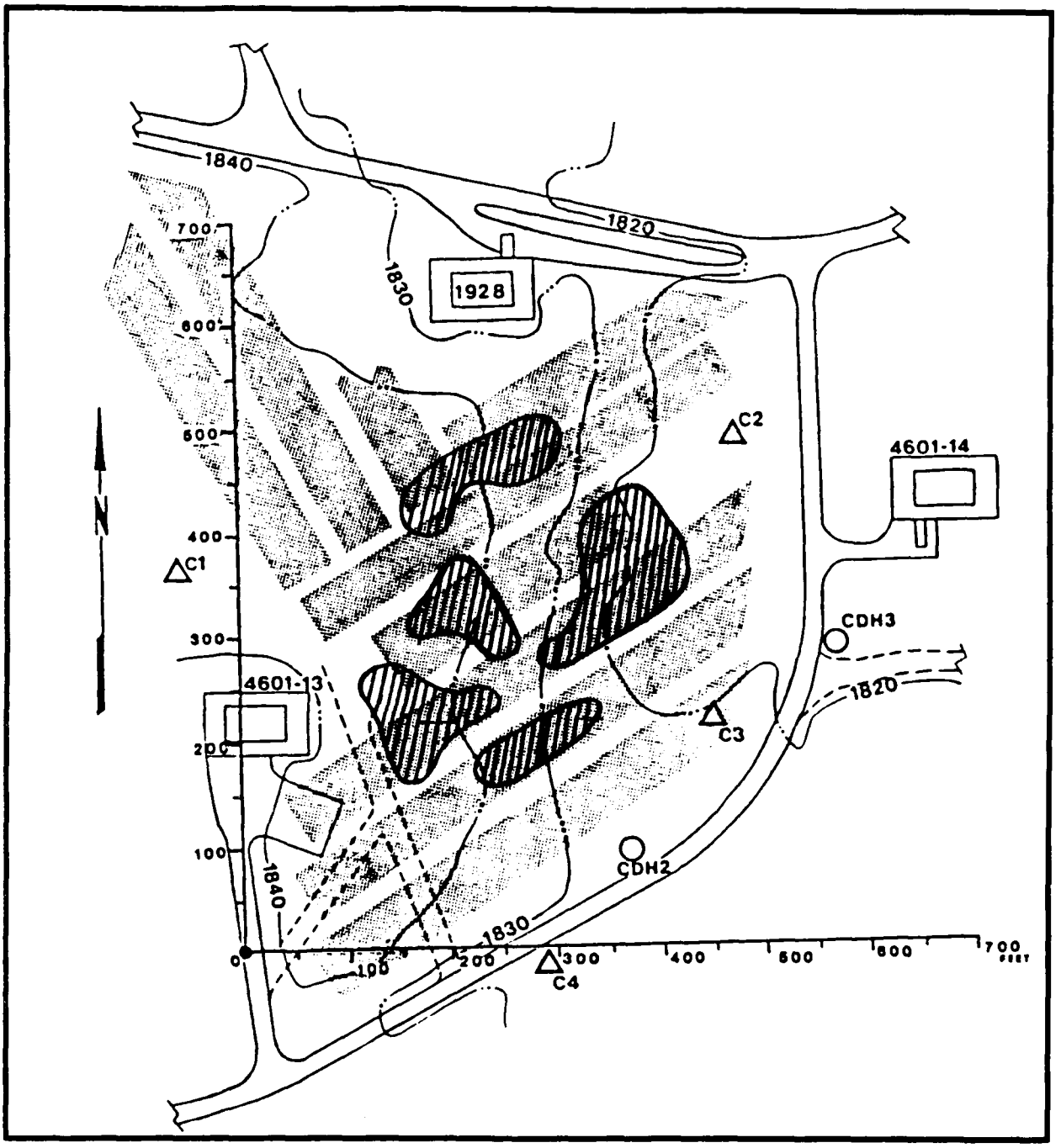

CDH3 C4 **Well Positions**

Actual Location of Landfill Cells

Interpreted Location of Landfill Cells -- (132 feet)

Figure 22. Interpreted location of landfill cells, 132 ft intercoil spacing, parallel orientation

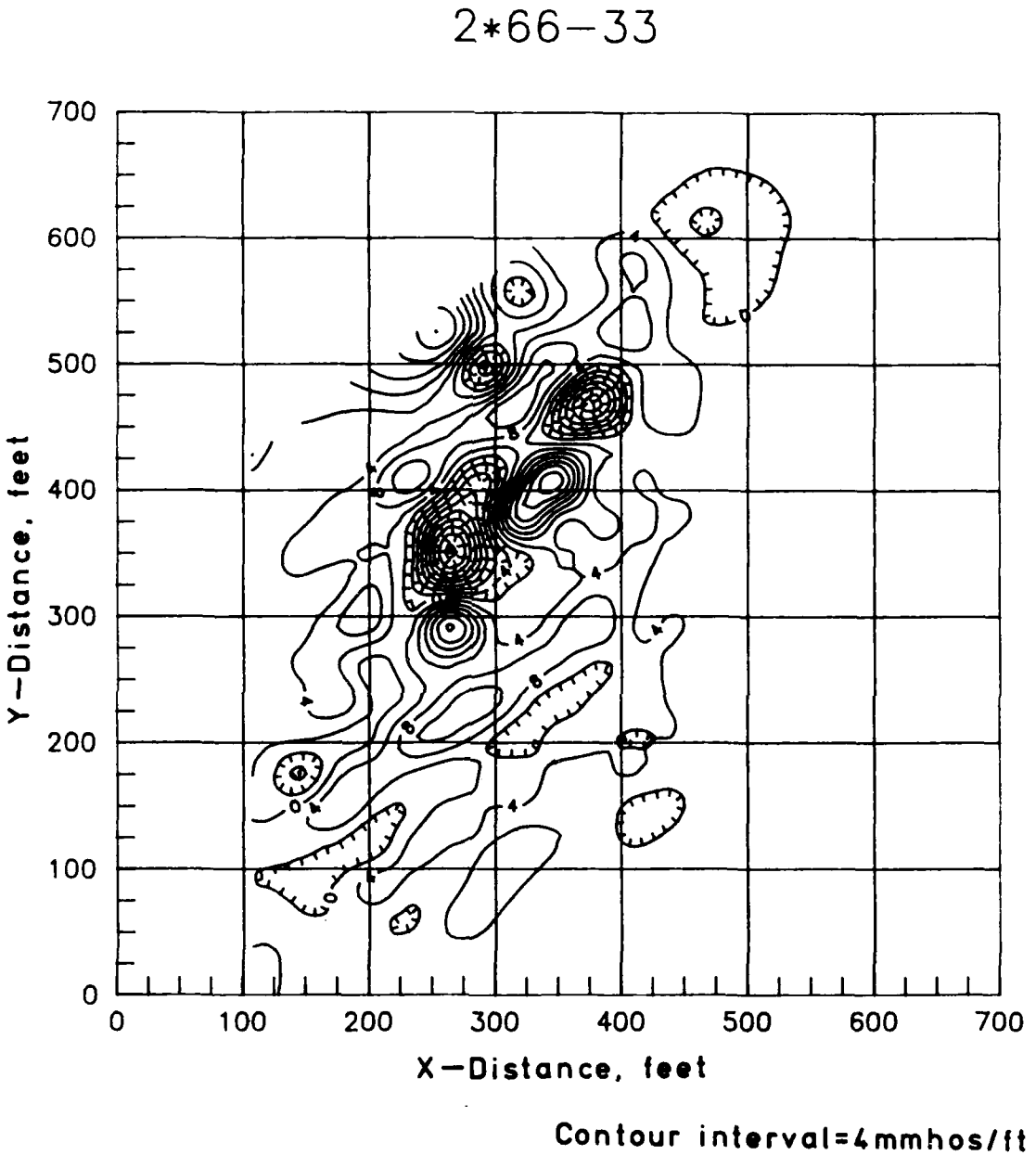

Figure 23. 2-D representation of two spacing method (2*C66 - C33), perpendicular orientation

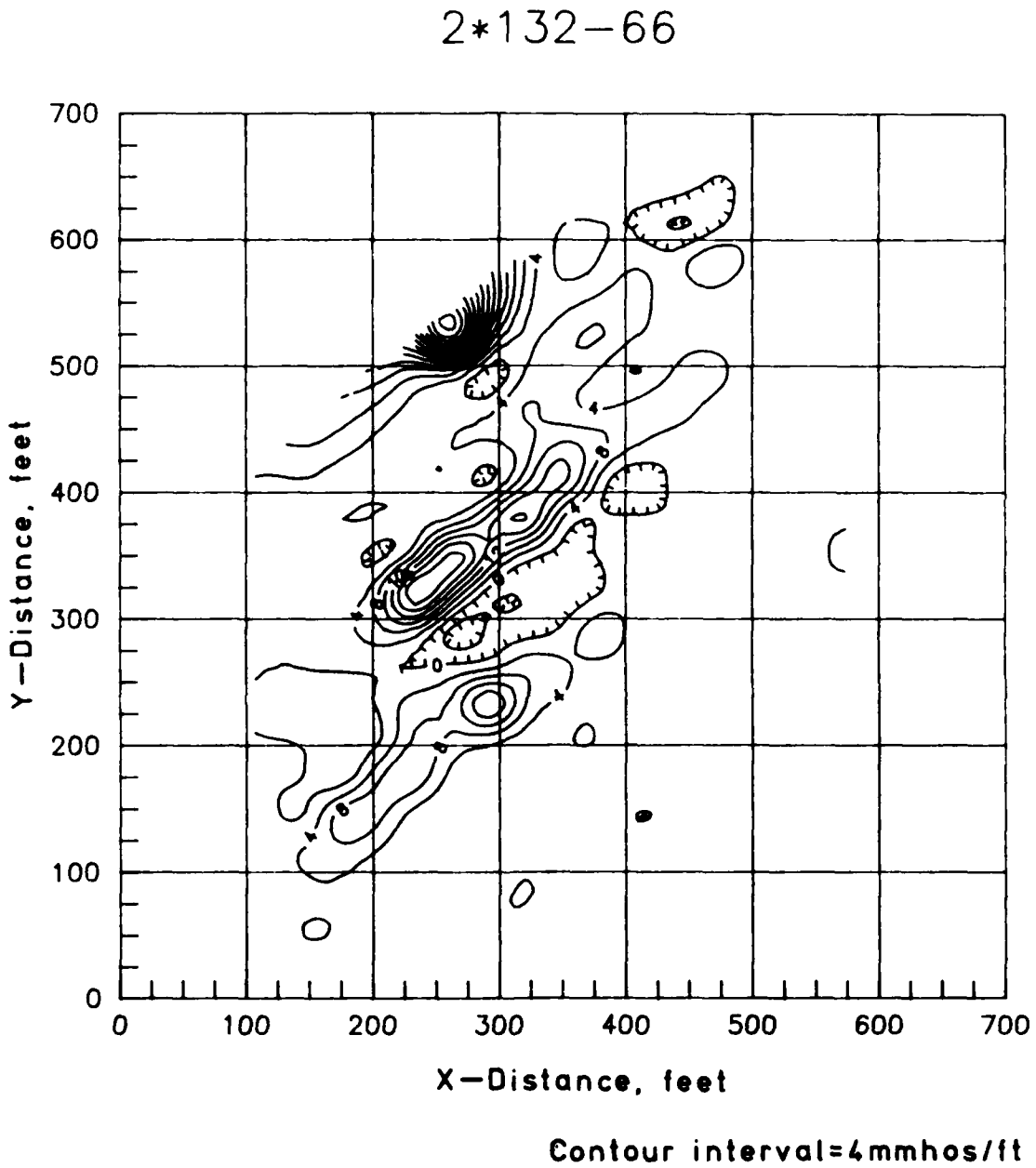

Figure 24. 2-D representation of two spacing method (2*C132 - C66), perpendicular orientation

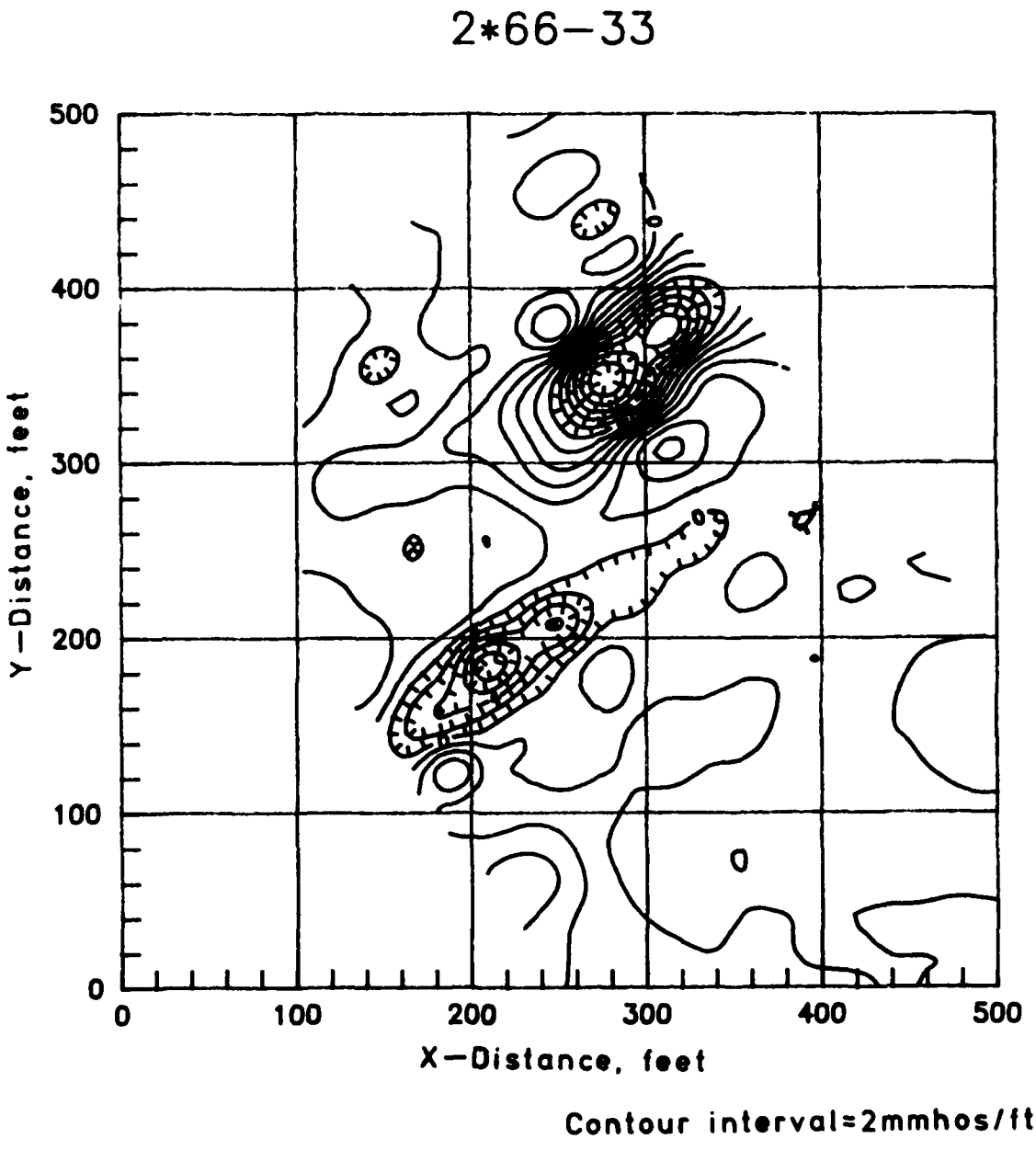

Figure 25. 2-D representation of two spacing method (2*C66 - C33), parallel orientation

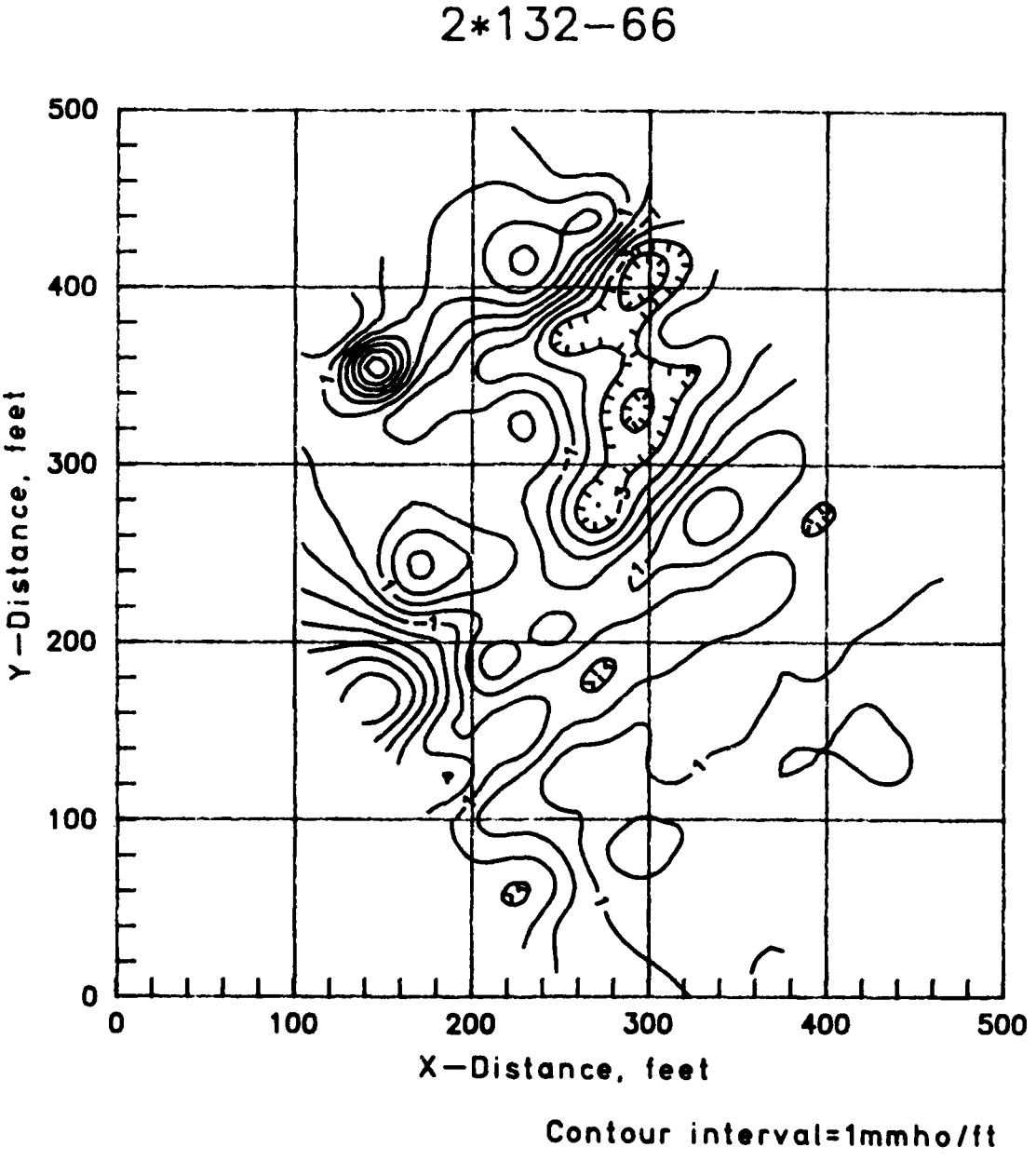

Figure 26. 2-D representation of two spacing method (2*C132 - C66), parallel orientation

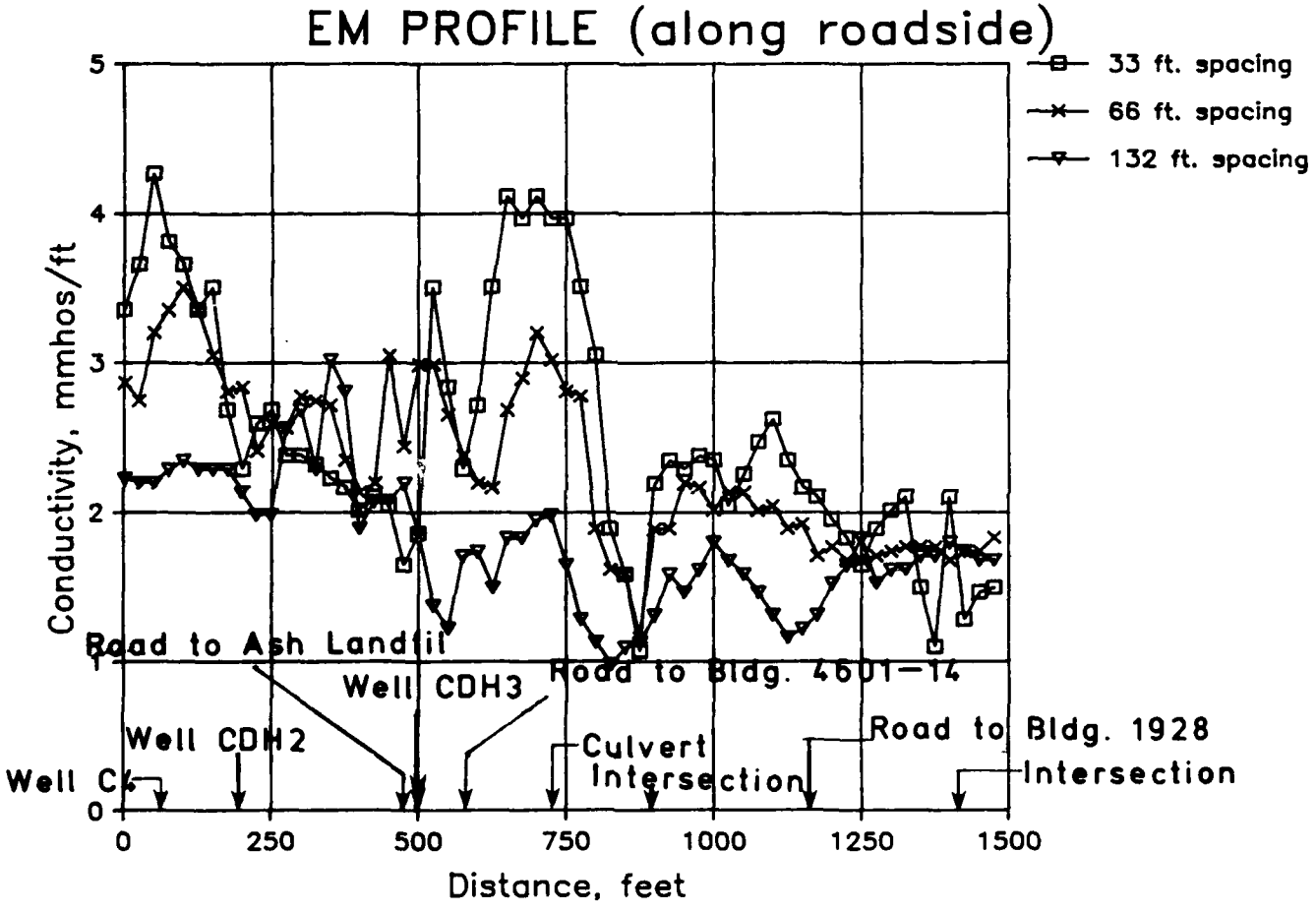

Figure 27. EM profile line along perimeter of HWMS-16

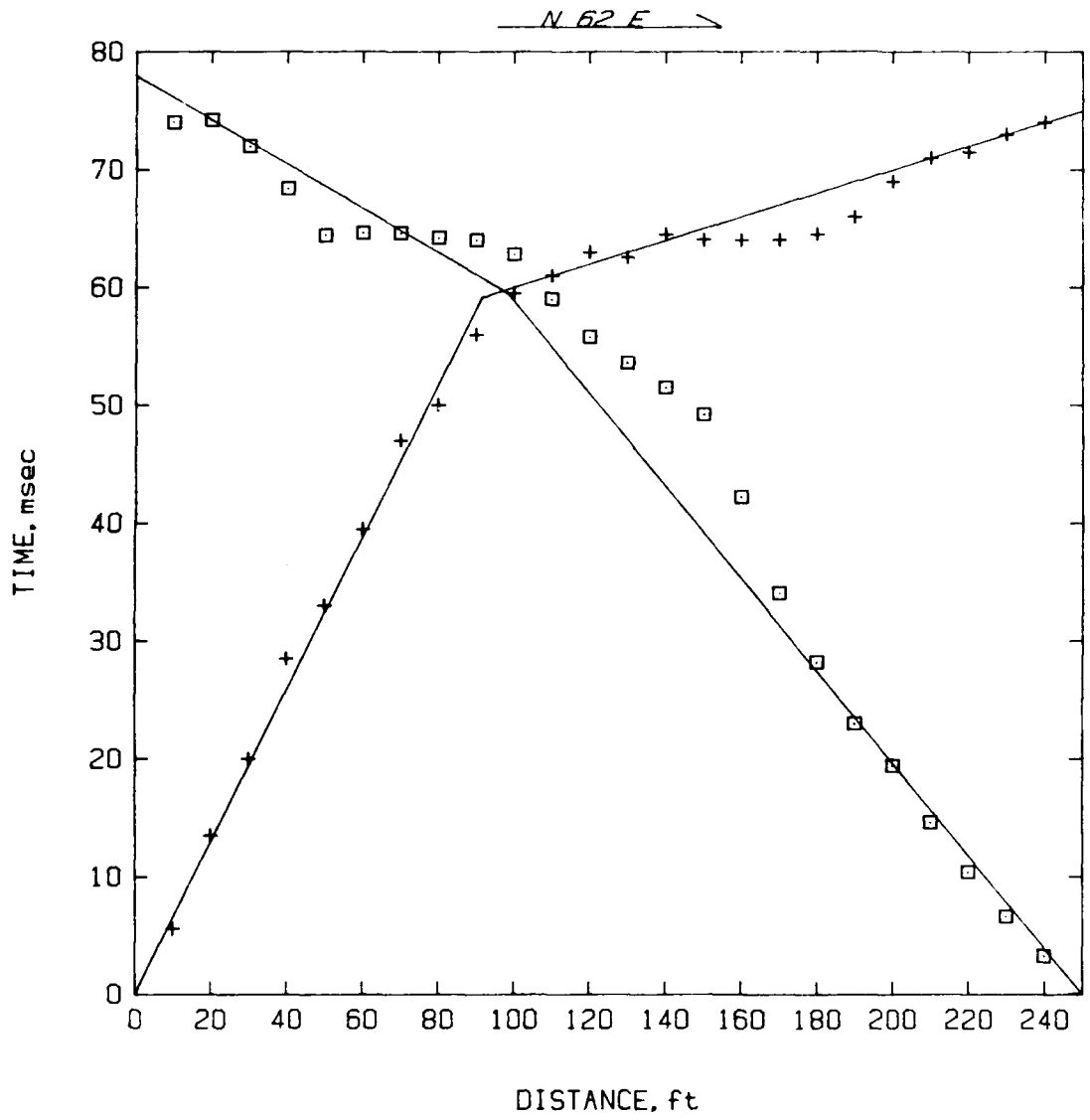

R-1

*** INPUT DATA ***

LAYER #	FORWARD VEL. FT/S	FORWARD TI. MSEC	REVERSE VEL. FT/S	REVERSE TI. MSEC
1	1550	0.0	2550	0.0
2	10000	50.0	5320	31.0

*** COMPUTED SEISMIC PROFILE ***

LAYER #	TRUE VEL. FT/S	DEPTH FOR. FT.	DEPTH REV. FT.
1	2050		
2	6910	54.0	33.5

Figure 28. Seismic refraction line R-1

R-2

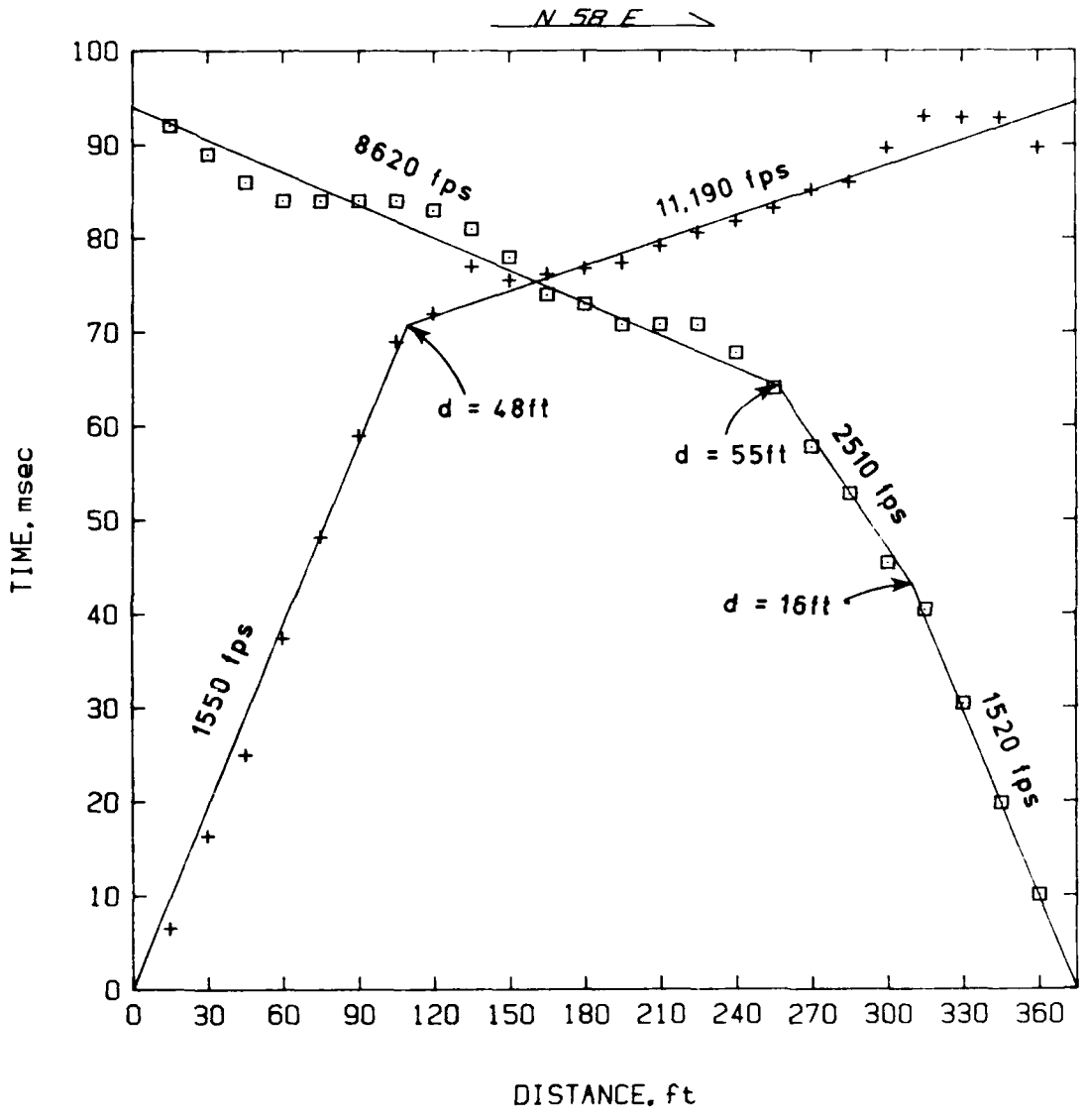

Figure 29. Seismic refraction line R-2

R-3

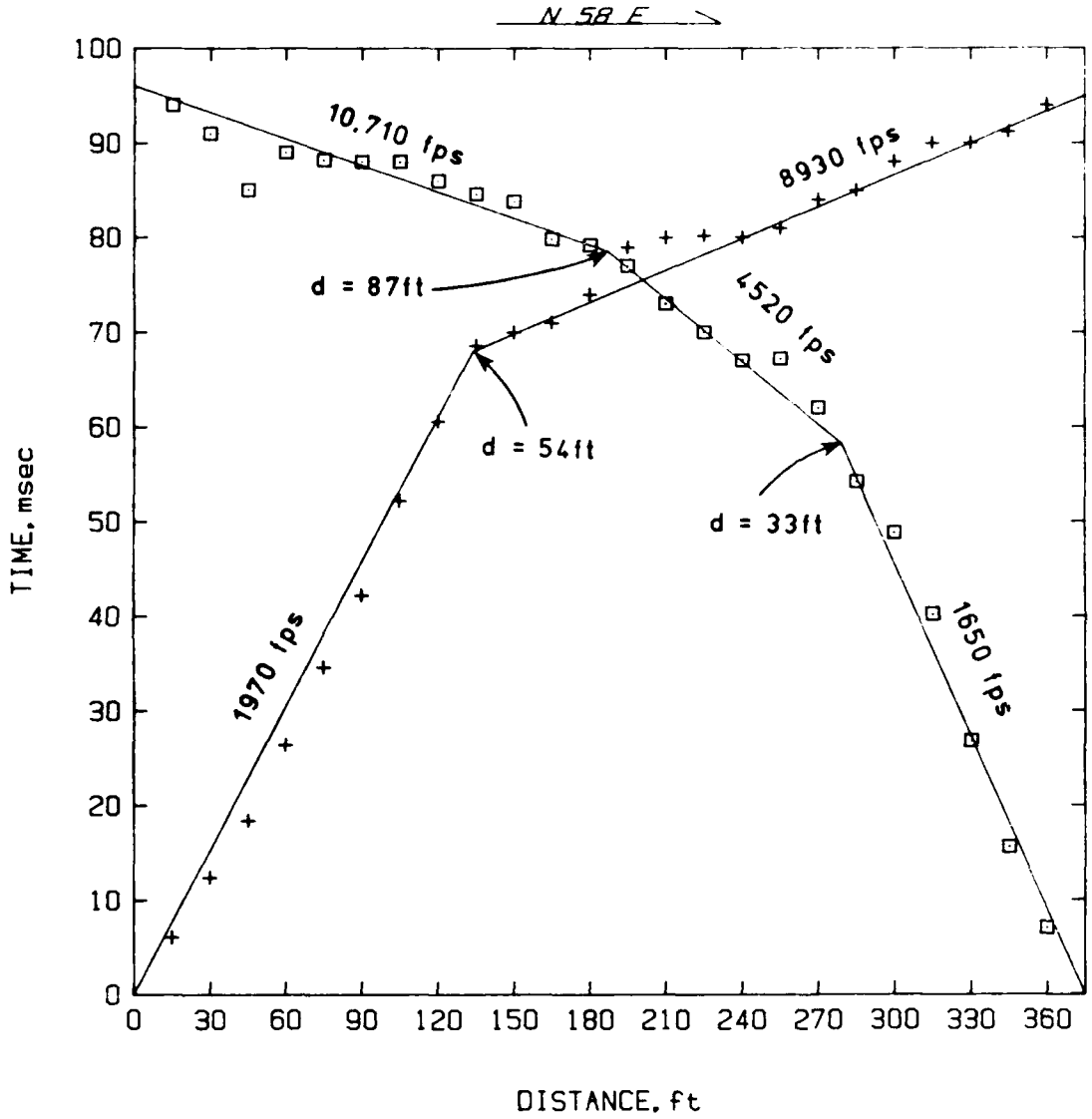

Figure 30. Seismic refraction line R-3

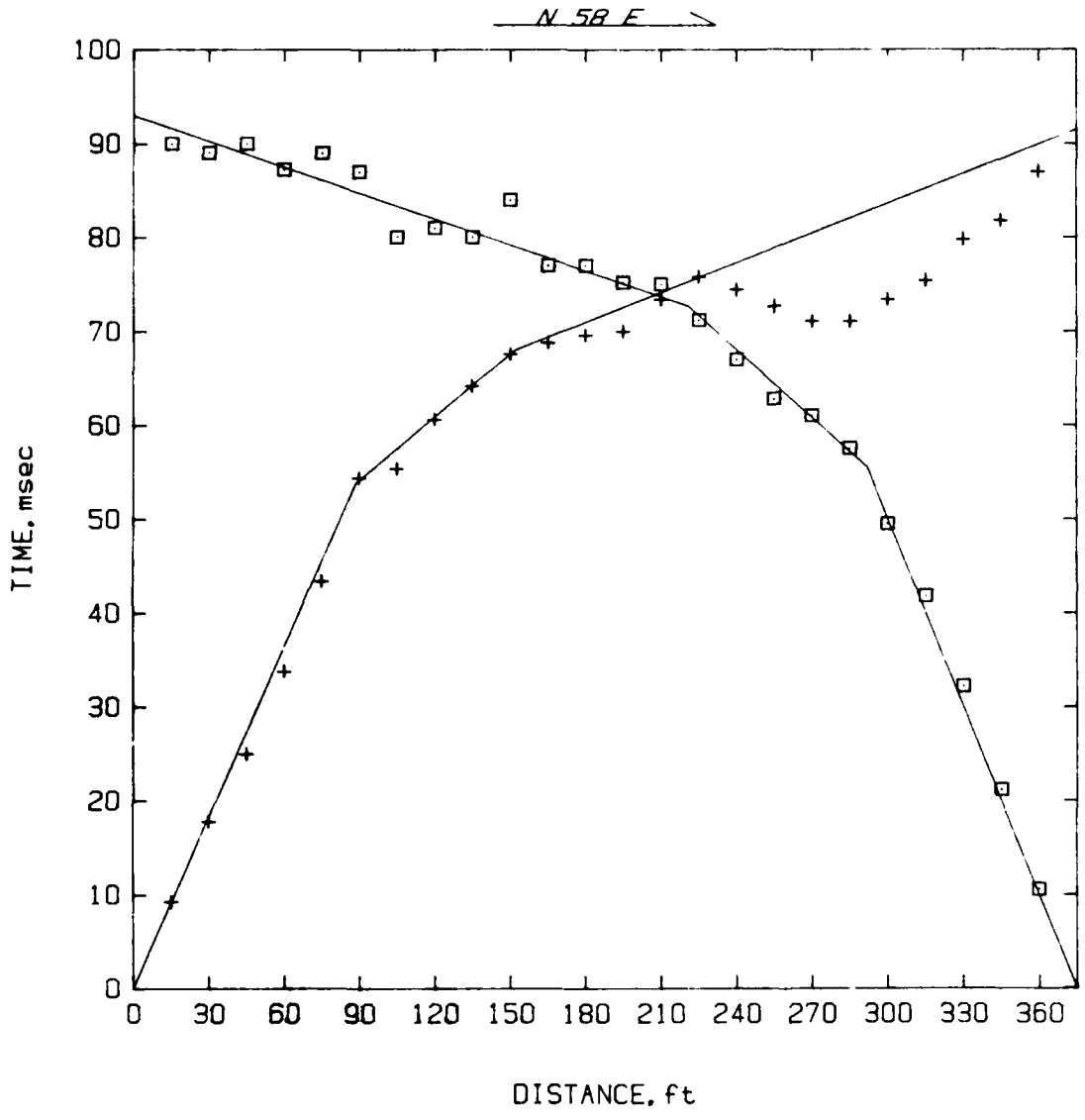

R-4

*** INPUT DATA ***

LAYER #	FORWARD VEL. FT/S	FORWARD TI. MSEC	REVERSE VEL. FT/S	REVERSE TI. MSEC
1	1650	0.0	1500	0.0
2	4470	34.0	4150	35.5
3	9490	52.0	10870	58.5

*** COMPUTED SEISMIC PROFILE ***

LAYER #	TRUE VEL. FT/S	DEPTH FOR. FT.	DEPTH REV. FT.
1	1580		
2	4300	29.0	30.0
3	10100	66.5	79.5

Figure 31. Seismic refraction line R-4

R-5

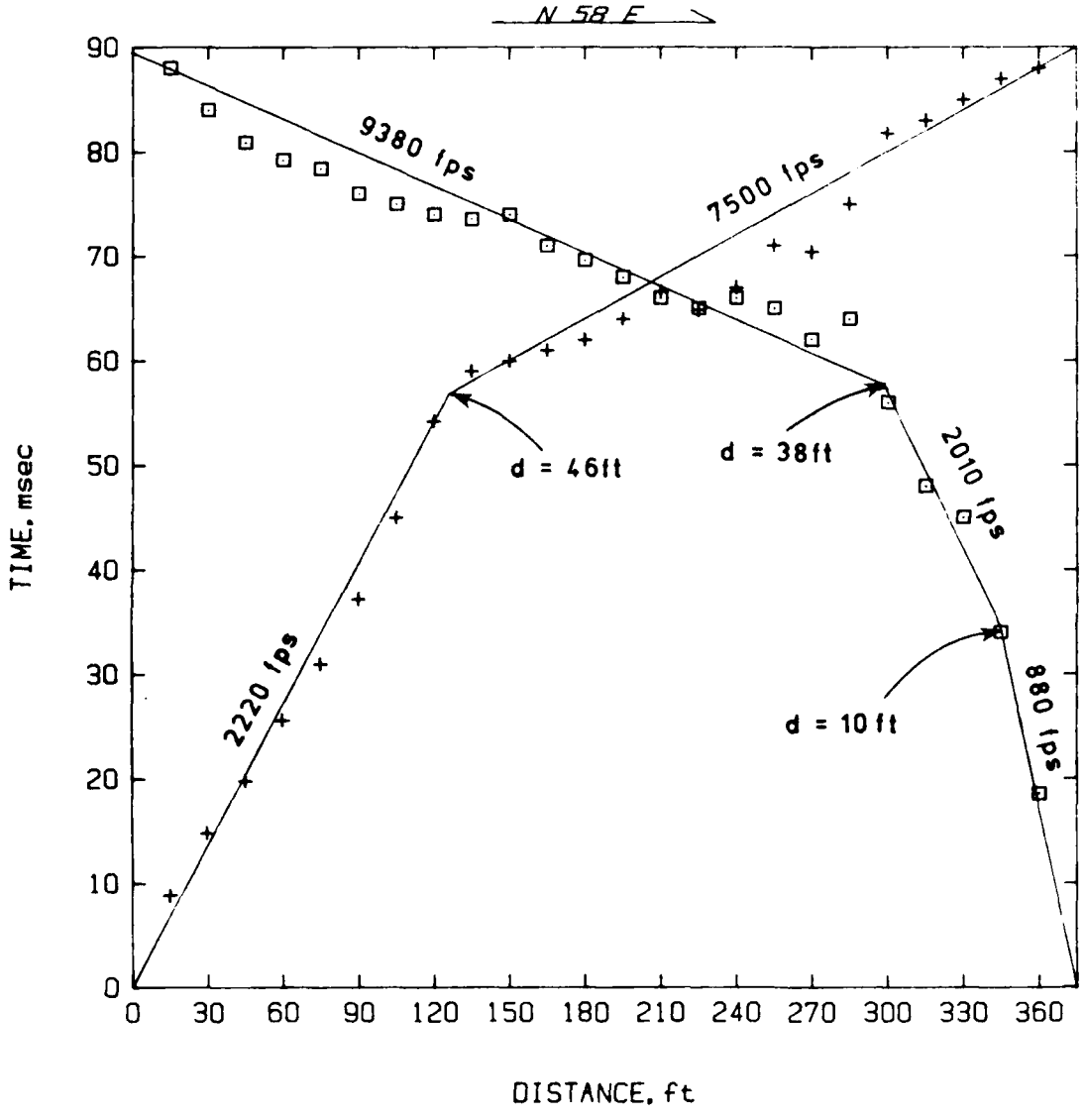

Figure 32. Seismic refraction line R-5

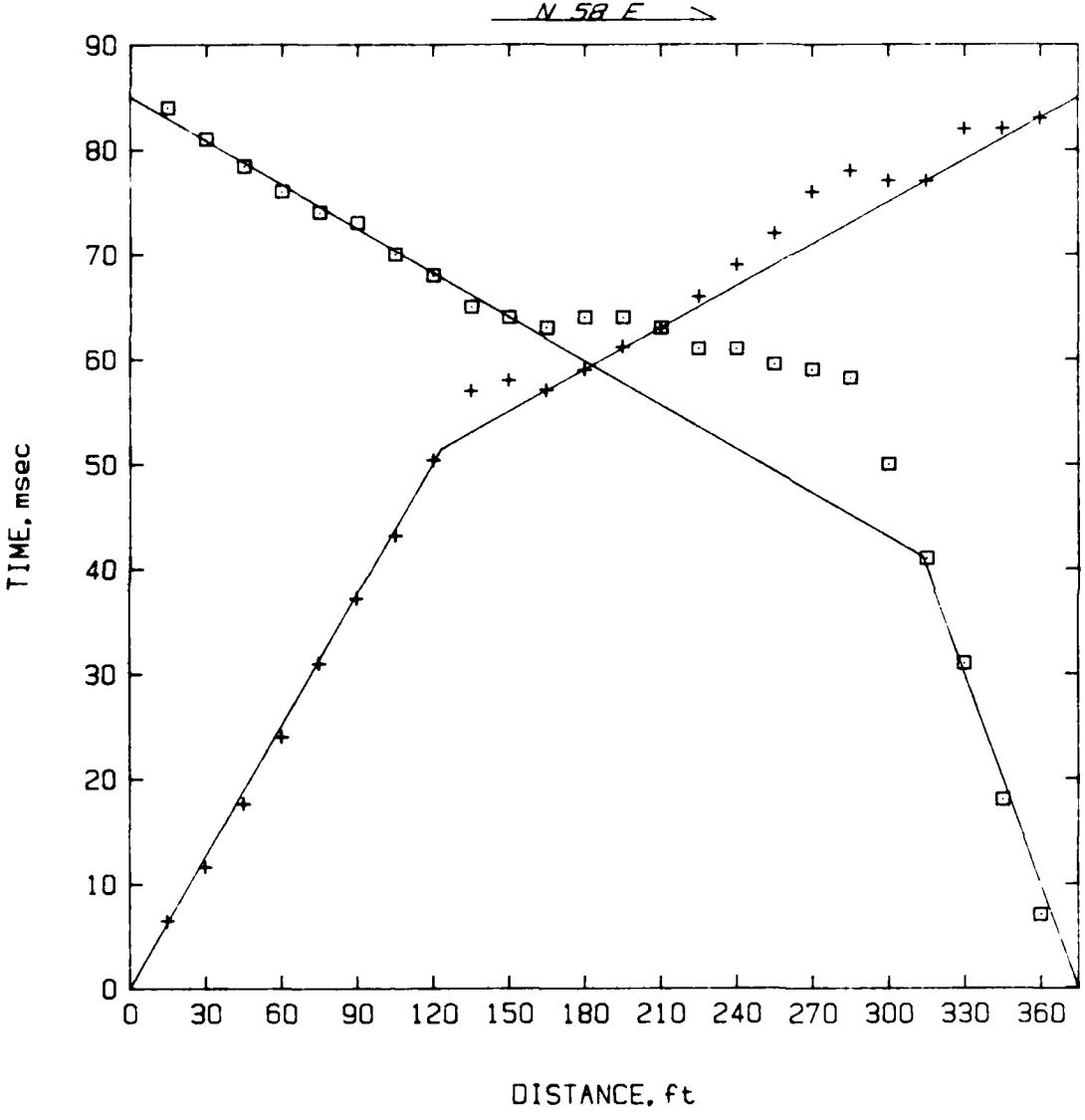

R-6

*** INPUT DATA ***

LAYER #	FORWARD VEL. FT/S	FORWARD TI. MSEC	REVERSE VEL. FT/S	REVERSE TI. MSEC
1	2400	0.0	1500	0.0
2	7500	35.0	7140	32.5

*** COMPUTED SEISMIC PROFILE ***

LAYER #	TRUE VEL. FT/S	DEPTH FOR. FT.	DEPTH REV. FT.
1	1950		
2	7310	35.5	33.0

Figure 33. Seismic refraction line R-6

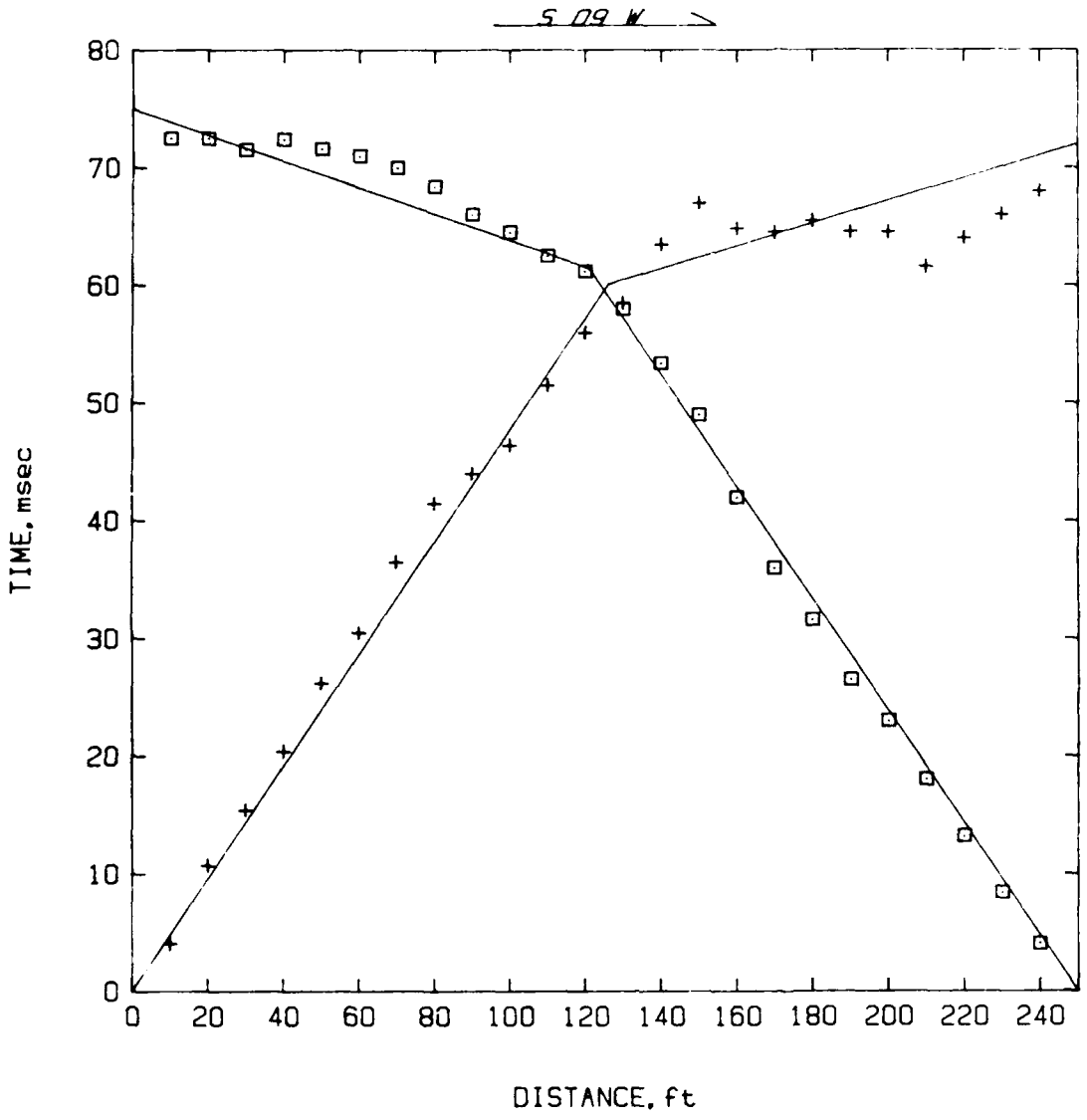

R-7

*** INPUT DATA ***

LAYER #	FORWARD VEL. FT/S	FORWARD TI. MSEC	REVERSE VEL. FT/S	REVERSE TI. MSEC
1	2100	0.0	2100	0.0
2	10420	48.0	8930	47.0

*** COMPUTED SEISMIC PROFILE ***

LAYER #	TRUE VEL. FT/S	DEPTH FOR. FT.	DEPTH REV. FT.
1	2100		
2	9810	51.5	50.5

Figure 34. Seismic refraction line R-7

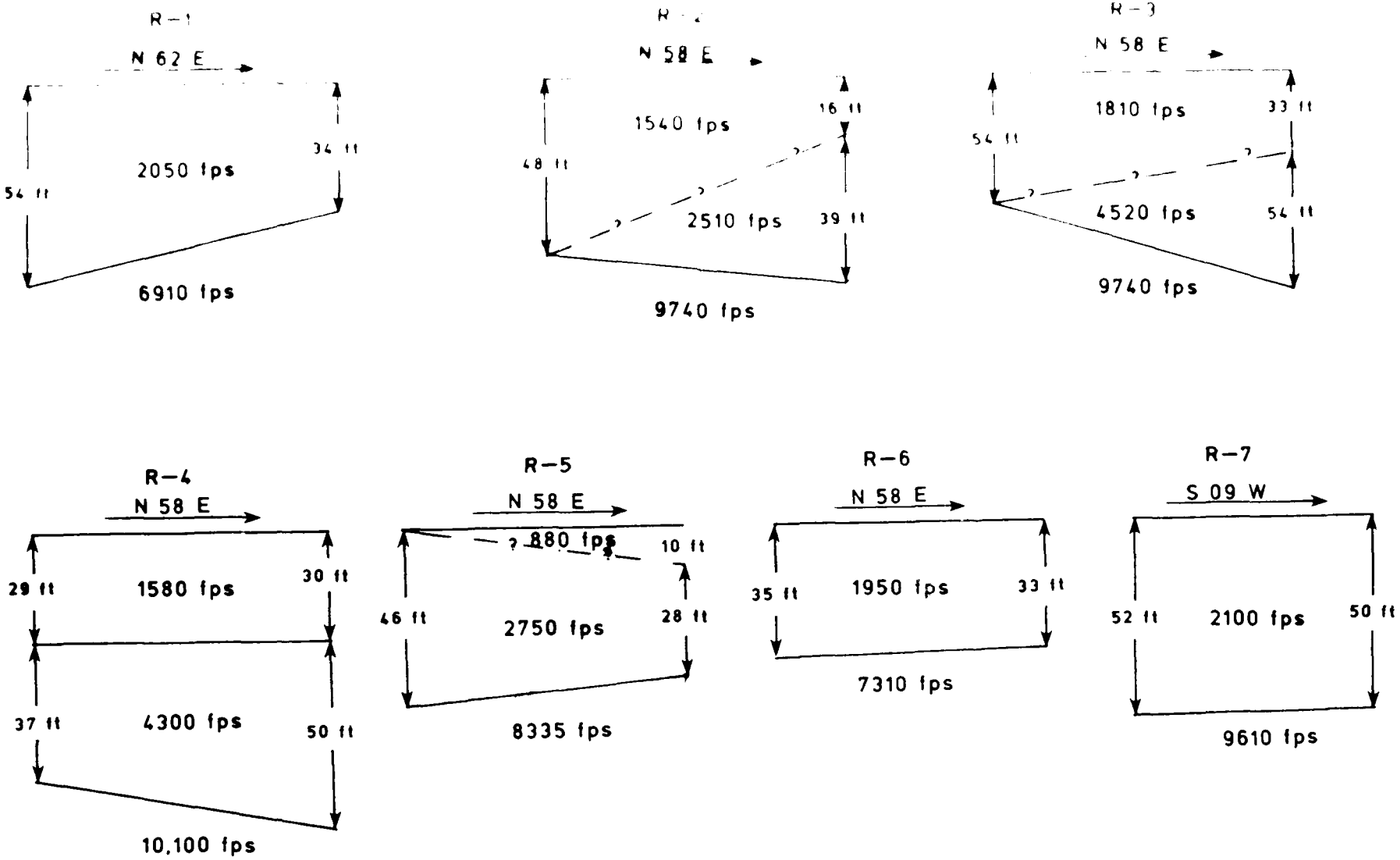

Figure 35. Summary of seismic refraction lines

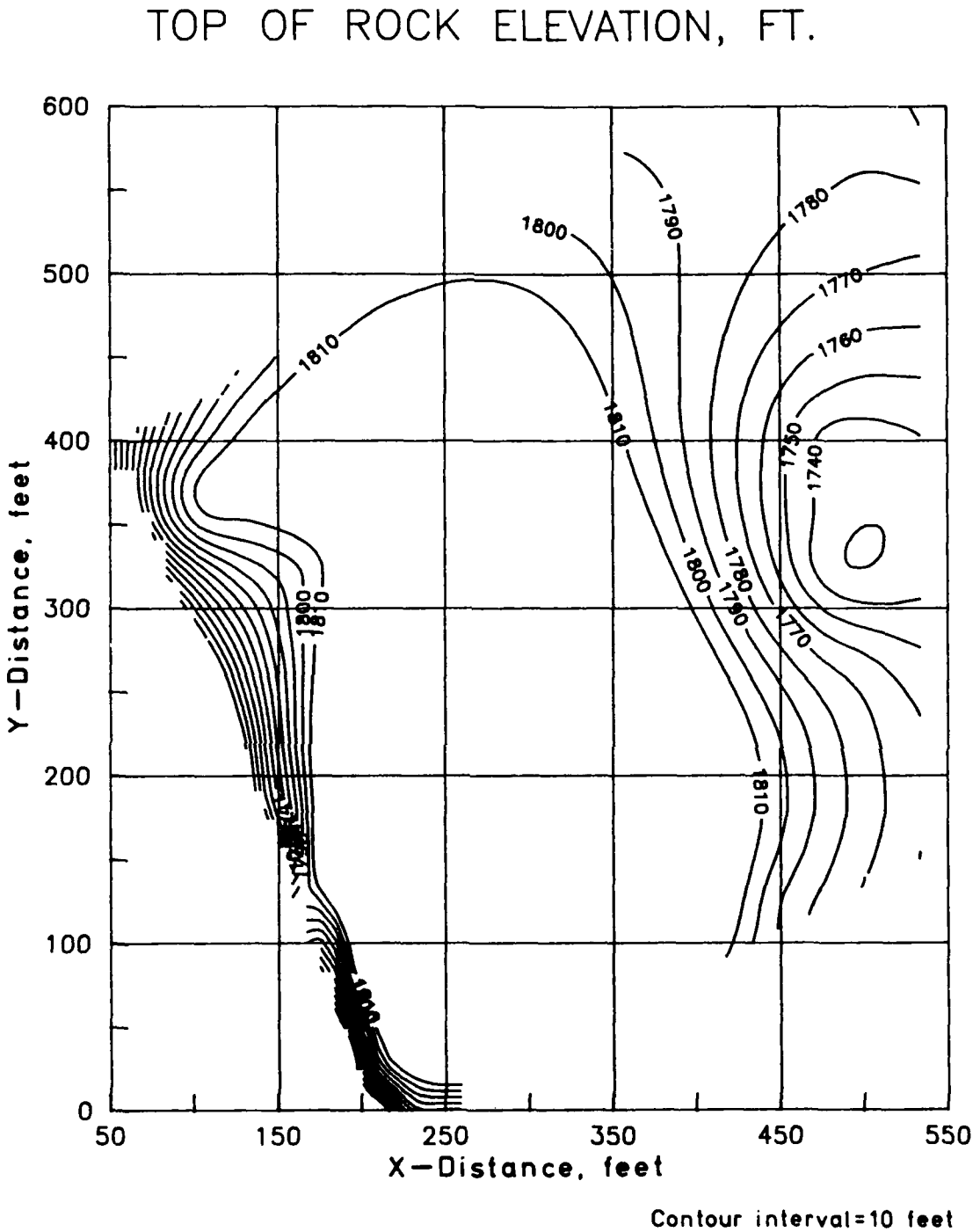

Figure 36. Top of rock elevation based on results of seismic refraction surveys